

SOURCE  
DATATRANSPARENT  
PROCESS

# Minor intron splicing is regulated by FUS and affected by ALS-associated FUS mutants

Stefan Reber<sup>1,2</sup>, Jolanda Stettler<sup>1,†</sup>, Giuseppe Filosa<sup>3,4</sup>, Martino Colombo<sup>1,2</sup>, Daniel Jutzi<sup>1</sup>, Silvia C Lenzken<sup>3</sup>, Christoph Schweingruber<sup>1,2</sup>, Rémy Bruggmann<sup>5</sup>, Angela Bachi<sup>4</sup>, Silvia ML Barabino<sup>3</sup>, Oliver Mühlemann<sup>1,\*\*</sup> & Marc-David Ruepp<sup>1,\*</sup>

## Abstract

Fused in sarcoma (FUS) is a ubiquitously expressed RNA-binding protein proposed to function in various RNA metabolic pathways, including transcription regulation, pre-mRNA splicing, RNA transport and microRNA processing. Mutations in the FUS gene were identified in patients with amyotrophic lateral sclerosis (ALS), but the pathomechanisms by which these mutations cause ALS are not known. Here, we show that FUS interacts with the minor spliceosome constituent U11 snRNP, binds preferentially to minor introns and directly regulates their removal. Furthermore, a FUS knockout in neuroblastoma cells strongly disturbs the splicing of minor intron-containing mRNAs, among them mRNAs required for action potential transmission and for functional spinal motor units. Moreover, an ALS-associated FUS mutant that forms cytoplasmic aggregates inhibits splicing of minor introns by trapping U11 and U12 snRNAs in these aggregates. Collectively, our findings suggest a possible pathomechanism for ALS in which mutated FUS inhibits correct splicing of minor introns in mRNAs encoding proteins required for motor neuron survival.

**Keywords** amyotrophic lateral sclerosis; FUS; minor intron splicing

**Subject Categories** Neuroscience; RNA Biology

**DOI** 10.15252/emboj.201593791 | Received 31 December 2015 | Revised 28 April 2016 | Accepted 29 April 2016

## Introduction

Dysfunctional RNA metabolism is implicated in a wide variety of neurodegenerative diseases, and many mutations leading to neurodegeneration have been identified in proteins with roles in RNA metabolism (Duan *et al*, 2014; Zhou *et al*, 2014). For example, mutations in the gene fused in sarcoma (FUS), which encodes an

ubiquitously expressed nuclear RNA-binding protein of the hnRNP family, were identified in patients with an inherited form of amyotrophic lateral sclerosis (ALS; Kwiatkowski *et al*, 2009; Vance *et al*, 2009). ALS is a fatal, adult-onset neurodegenerative disease that selectively kills brain and spinal cord motor neurons. While most cases appear to be sporadic (sALS), 10% of cases are inherited (familial ALS, fALS). Approximately 4–5% of fALS and some sALS cases are due to mutations in FUS (Lagier-Tourenne & Cleveland, 2009; DeJesus-Hernandez *et al*, 2010).

Fused in sarcoma mRNA consists of 15 exons encoded on chromosome 16 (Aman *et al*, 1996) and gives rise to a 526-amino acid-long protein. The FUS protein contains a prion-like N-terminal glutamine, glycine, serine and tyrosine rich (Q/G/S/Y) domain, which is conserved within the FET family of proteins (FUS, EWS and TAF15) and is required for homo- or heterodimer formation among them. Furthermore, FUS contains three arginine/glycine/glycine (RGG<sub>1-3</sub>) domains, a RNA recognition motif (RRM) and a zinc finger (Zn). These domains were associated with DNA and RNA binding. Furthermore, FUS comprises a predicted nuclear export signal (NES) embedded in the RRM and a C-terminal nuclear localization signal (NLS) (Iko *et al*, 2004; Kwiatkowski *et al*, 2009; Dormann *et al*, 2010; Thomsen *et al*, 2013).

Most reported FUS-linked ALS-causing mutations are missense mutations clustered in the highly conserved C-terminal NLS (Dormann *et al*, 2010). Depending on the mutation, this leads to almost abolished or significantly reduced nuclear import of FUS and to the formation of FUS aggregates in the cytoplasm of neurons and glial cells of ALS patients (Bentmann *et al*, 2013), indicating that these mutations either lead to a loss of function in the nucleus, to a gain of function in the cytoplasm or to a combination of both (Wang *et al*, 2013; Sun *et al*, 2015).

Fused in sarcoma has been implicated to function in several steps of gene expression. It regulates the transcription through the interaction with RNA polymerases (RNAP) II and III and several transcription factors (Uranishi *et al*, 2001; Li *et al*, 2010; Tan & Manley,

1 Department of Chemistry and Biochemistry, University of Bern, Bern, Switzerland

2 Graduate School for Cellular and Biomedical Sciences, University of Bern, Bern, Switzerland

3 Department of Biotechnology and Biosciences, University of Milano-Bicocca, Milan, Italy

4 IFOM-FIRC Institute of Molecular Oncology, Milan, Italy

5 Interfaculty Bioinformatics Unit and Swiss Institute of Bioinformatics, University of Bern, Bern, Switzerland

\*Corresponding author. Tel: +41 31 631 4348; E-mail: marc.ruepp@dcb.unibe.ch

\*\*Corresponding author. Tel: +41 31 631 4627; E-mail: oliver.muehlemann@dcb.unibe.ch

†Present address: Interregionale Blutspende SRK AG, Bern, Switzerland

2010; Schwartz *et al*, 2012). Besides its functions in transcription, FUS was also identified as a splicing regulator based on its presence in spliceosomal complexes (Rappsilber *et al*, 2002; Zhou *et al*, 2002) and interactions with several splicing factors (Meissner *et al*, 2003) as well as with the U1 snRNP (Hackl *et al*, 1994; Yamazaki *et al*, 2012; Gerbino *et al*, 2013; Yu *et al*, 2015). Recent CLIP studies showed that FUS binds to nascent transcripts of many different pre-mRNAs, preferentially to long introns (Hoell *et al*, 2011; Rogelj *et al*, 2012), and splicing analysis in the embryonic brains of FUS-knockout mice revealed splicing changes in more than 300 genes (Lagier-Tourenne *et al*, 2012). However, the molecular mechanism by which FUS influences pre-mRNA splicing remained so far unknown.

To address the roles of FUS in RNA metabolism, we performed mass spectrometric analysis to identify high-confidence interactors of FUS. We found that minor spliceosome components are highly enriched among the FUS-interacting proteins. In line with this finding, FUS knockout affects predominantly the removal of minor introns. We subsequently confirmed that FUS is necessary for the efficient splicing of a subset of minor intron-containing mRNAs (so-called U12-type introns), among them members of the voltage-gated sodium channel family that are required for proper muscle function and post-natal maturation of spinal motor neurons (Jurkat-Rott *et al*, 2010; Porter *et al*, 1996). Our data reveal that FUS directly regulates the removal of minor introns through the direct interactions with the minor spliceosome at the 5' splice site of these introns. We further show that the ALS-associated FUS-P525L mutation, which destroys the NLS and results in cytoplasmic retention of FUS (Dormann *et al*, 2010), fails to promote the efficient splicing of minor introns and causes mislocalization of the minor spliceosome components U11 and U12 snRNA to the cytoplasm. Collectively, our findings identify a role of FUS in splicing of minor introns, many of which occur in genes with neuronal functions, and imply that a loss of this nuclear function might contribute to the development of ALS. Intriguingly, our results suggest a possible mechanistic link between FUS-linked and TDP-43-linked ALS, as well as spinal muscular atrophy (SMA) in the light that all three neurodegenerative diseases exhibit a diminished minor spliceosome function (Lotti *et al*, 2012; Ishihara *et al*, 2013).

## Results

### Identification of FUS-interacting proteins

In order to unravel the molecular pathways involving FUS, a mass spectrometry-based interactome analysis was performed. Since FUS binds RNA (Zinszner *et al*, 1997), the interactome analysis was carried out with or without RNase treatment of the cell lysates to distinguish between protein-to-protein interactions and interactions mediated by RNA. Immunoprecipitations (IPs) were performed from HEK293T cell lysates transiently expressing Flag-tagged wild-type FUS or Flag-EBFP (enhanced blue fluorescent protein) as a control (Fig 1A). While the control IPs were essentially devoid of co-precipitating proteins (lanes 3, 5 and 7), many proteins were detected on a Coomassie-stained gel in the Flag-FUS IP performed under low stringency conditions (150 mM NaCl washes) and in the absence of RNase (lane 4). Treatment of the lysates with RNase A

prior to the IP reduced the number of bands, indicating that many interactions are RNA-mediated (compare lanes 4 and 6). Repetition of the IPs with RNase-treated lysates under more stringent washing conditions (750 mM NaCl) to identify those proteins that associated with FUS with the highest affinity further reduced the number of detectable bands on the gel (lane 8).

The gel lanes were then excised and processed for in-gel tryptic digestion before liquid chromatography–tandem mass spectrometry analysis (LC-MS/MS). Proteins detected in the control IP, which represent unspecific interactors with the anti-Flag matrix, were eliminated from further analysis. A total of 587 potential interactors were identified, 444 of which were only detected under low stringency conditions and in the absence of RNase, and 97 of those were also identified in the RNase-treated sample (Fig 1B). Of these 97 proteins, 40 were even detected under high stringency conditions, identifying them as relatively stable and RNA-independent interactors of FUS with high confidence. The results derive from two biological replicates for each condition and only proteins detected in both were considered. The proteins identified under all three conditions are listed in Appendix Table S1.

Gene ontology (GO) analysis was performed for the 40 proteins co-immunoprecipitating with FUS under all three conditions to reveal the most enriched biological processes and cellular components involving these genes. Statistically highly significantly enriched were biological processes related to RNA metabolism, in particular RNA splicing (Fig 1C). This aspect is also evident in the cellular component analysis, where the terms “spliceosomal complex” and “U12-type spliceosomal complex” are highly enriched (Fig 1D).

### FUS interacts with the U11 snRNP

Because of the GO analysis pointing towards spliceosomal complex and previous evidence for an interaction of FUS with U1 snRNP (Hackl *et al*, 1994; Yamazaki *et al*, 2012; Sun *et al*, 2015; Yu *et al*, 2015), we performed RNA-IPs from HeLa nuclear extract using anti-FUS antibodies, or anti-BSA antibodies as negative control, followed by RT-qPCR to test for U snRNA enrichment. Consistent with the published data, U1 snRNA was strongly enriched in the FUS IP. Intriguingly, and in line with the GO analysis of the mass spectrometry results (Fig 1D), the most enriched U snRNA was the U11 snRNA, a member of the minor spliceosome (also called U12-type spliceosome) and constituent of the U11/U12 di-snRNP (Fig 2A and Appendix Fig S1A). These results are in accordance with the previous findings reporting the presence of FUS in the human spliceosomal complexes E, A and B, in which the U1 and U11 snRNPs are present, but not in the B<sup>act</sup> and C complexes, a stage at which U1 and U11 snRNPs have left the pre-mRNA (Hartmuth *et al*, 2002; Deckert *et al*, 2006; Behzadnia *et al*, 2007). The results further indicate that the observed enrichment of U5 snRNA in our FUS-RNA-IPs is unlikely to be direct, because U5 snRNA is present throughout the entire splicing cycle, whereas FUS is confined to the early spliceosome assembly stages (Will & Luhrmann, 2011). We therefore did not further investigate the U5 snRNA association with FUS, but instead focused on the interaction of the minor spliceosome component U11 snRNA with FUS.

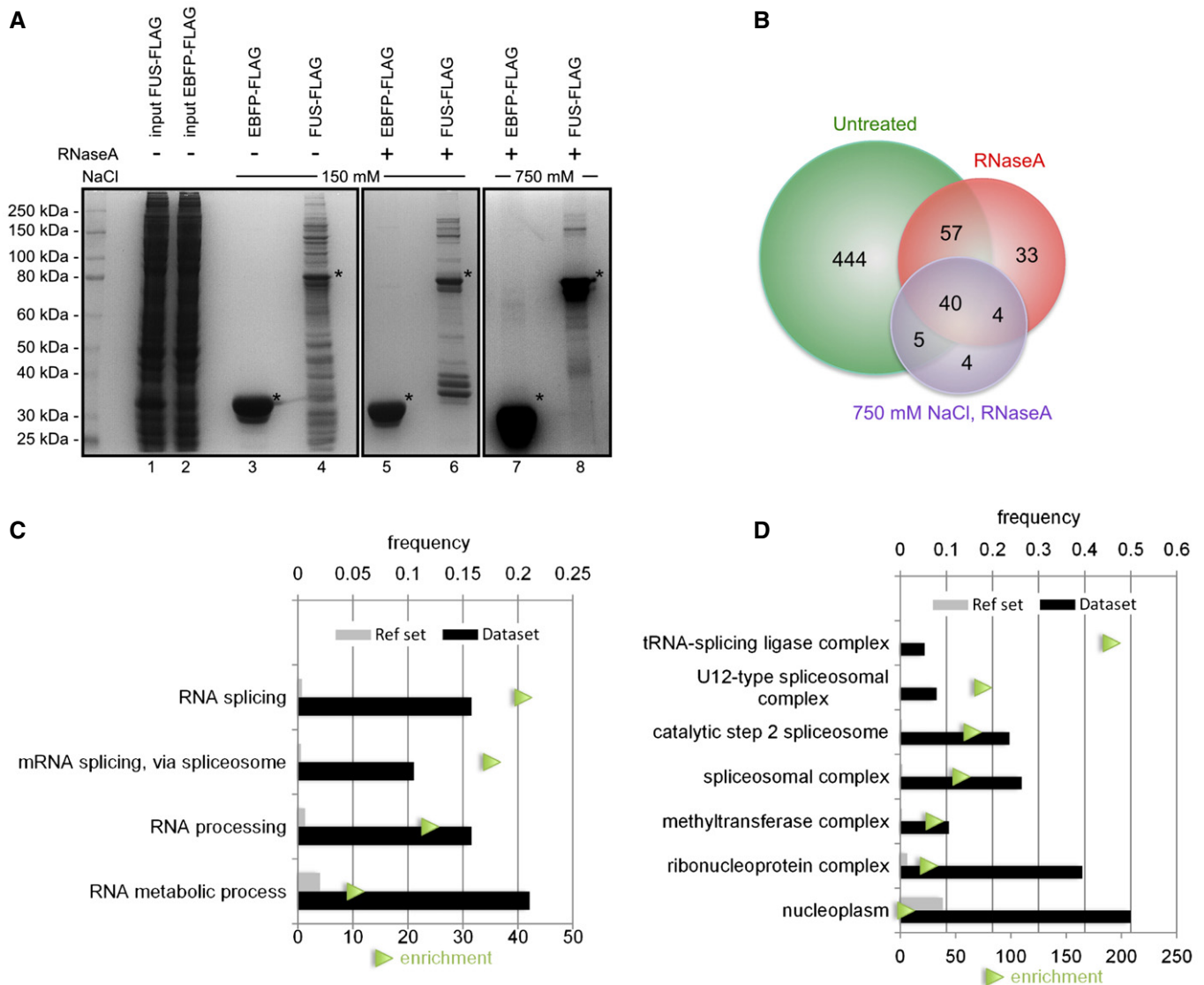


**Figure 1. Mass spectrometric identification of FUS-interacting proteins.**

A FLAG-tagged FUS and EBFP (negative control) were immunoprecipitated from the total cell extracts of 293T cells under low stringency (150 mM NaCl) without (lanes 3–4) or with RNase A treatment (lanes 5–6) as well as with RNase A treatment and immunoprecipitation with high stringency washes (750 mM NaCl, lanes 7–8). Purified protein complexes were eluted from the anti-FLAG affinity gel by FLAG peptide, separated by SDS-PAGE and stained with Coomassie. Asterisks indicate the baits (FUS-FLAG and EBFP-FLAG).

B Venn diagram representing the overlap of the proteins identified under low stringency (with [red] and without RNase A treatment [green]) and high stringency conditions (purple).

C Gene ontology enrichment analysis of the 40 high-confidence interactors of FUS according to biological process.

D Gene ontology enrichment analysis of these FUS interactors according to the cellular component. Frequency refers to the percentage of FUS-interacting proteins annotated to a certain GO term in the data set (black bar) and in the human reference set (grey bar). The enrichment value (green triangles) represents the ratio between the frequencies of the specific term in the FUS IPs and in the human genes reference data set. All terms are significantly enriched with a *P*-value < 0.05.

The interaction of FUS with U11 snRNP was validated by performing pull-downs using biotinylated antisense oligonucleotides against U11 snRNA. The U11 snRNP pull-downs were not only enriched for the U11/U12 di-snRNP-specific factor U11-59K and the common spliceosomal Sm ring component Smd3, but also for FUS and for hnRNP H (Fig 2B). hnRNP H is required for optimal U11 snRNP binding to certain transcripts (McNally *et al*, 2006) and is one of the conserved FUS interactors (Appendix Table S1,

Appendix Fig S1B). In agreement with the previously published data (Sun *et al*, 2015), we also co-purified FUS in U1 snRNP pull-downs (Appendix Fig S2).

To confirm that these interactions take place *in situ* and do not arise from rearrangements in the extracts after cell lysis, we performed proximity ligation assays (PLA): HeLa cells fixed with paraformaldehyde and permeabilized with Triton X-100 were incubated with antibodies recognizing FUS together with antibodies

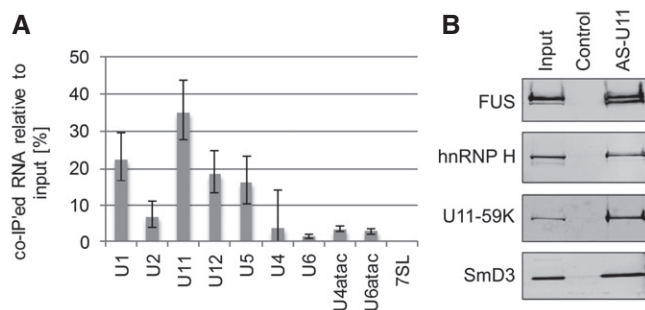


**Figure 2. FUS interacts with the U11 snRNP.**

**A** HeLa nuclear extracts were subjected to immunoprecipitation with anti-FUS antibodies or BSA antibodies (negative control) and the co-precipitated snRNAs as well as 7SL RNA were quantitated by RT-qPCR. The respective RNA amounts detected in the IPs are expressed as percentage of the input. The precipitated RNA levels measured in the negative control were subtracted from those in the FUS-RNA-IP. The data before background subtraction are shown in Appendix Fig S1. Error bars indicate standard deviations (SD) of three biological replicates, each measured in duplicate.

**B** Enrichment of FUS after U11 snRNP affinity purification with a biotinylated antisense oligonucleotide (AS-U11) complementary to U11 snRNA from HeLa nuclear extracts. As control, incubation of the magnetic streptavidin beads with AS-U11 was omitted. After biotinylated antisense oligonucleotide pull-down, the purified complexes were eluted from the beads and subjected to 4–12% NuPAGE gels. The blots were incubated with mouse anti-FUS-IRDye800CW, goat anti-hnRNP H, rabbit anti-U11-59K and rabbit anti-SmD3, followed by the detection with species-specific IRDye680LT- or IRDye800CW-labelled secondary antibodies to confirm the presence of FUS, hnRNP H, U11-59K and SmD3 in the AS-U11-enriched fraction. Input corresponds to 9% of the used material for pull-down.

directed against U1 snRNP and U11/U12 di-snRNP-specific proteins, respectively (Appendix Fig S3). The PLA confirmed that FUS colocalized in cells within < 40 nm distance to U1 snRNP-specific factors U1A and U1C as well as to the U11/12 di-snRNP-specific proteins U11-59K and U11-31K, consistent with the observed association of FUS with the U1 and the U11/12 di-snRNP.

### Expression and splicing of minor intron-containing genes is strongly disturbed in the absence of FUS

To test the influence of FUS on gene expression and splicing at a genome-wide level and to identify the potential targets of FUS, we generated FUS-knockout SH-SY5Y (FUS KO SH-SY5Y) cells and assessed the alterations in splicing by high-throughput sequencing. These FUS KO SH-SY5Y cells were generated by targeting the first intron of the FUS gene with CRISPR/Cas9 and co-transfection of a donor plasmid harbouring a Zeocin resistance cDNA for homologous recombination. The Zeocin cDNA is preceded by a chimeric intron containing the strong 3' splice site from the rabbit  $\beta$ -globin intron 2, resulting in the in-frame splicing of the FUS exon 1 to the Zeocin cassette. The Zeocin cassette is followed by the strong SV40 polyadenylation signal that leads to premature polyadenylation of the FUS mRNA and the expression of the Zeocin resistance marker (Fig 3A). The absence of FUS mRNA isolated from individual Zeocin-resistant cell clones was verified by RT-qPCR (data not shown), and for the two selected FUS KO clones, the absence of FUS protein was demonstrated by Western blotting (Fig 3B). From these

two clonal cell lines and from wild-type SH-SY5Y cells, we then extracted total RNA and performed mRNA-seq.

The sequencing data confirmed that in the FUS KO cells, transcription of the FUS gene is terminated as intended in intron 1 where the artificial Zeocin-encoding exon with the SV40 polyadenylation signal was introduced (Fig 3C). To address whether minor intron-containing genes are differentially expressed in the FUS KO SH-SY5Y cells, we performed a gene-level analysis on the mRNA-seq data. Among the differentially expressed genes, those harbouring a minor intron were indeed enriched (Fig 4A). Two-thirds of the differentially expressed minor intron-containing genes were downregulated and one-third was upregulated, respectively (Fig 4B and Appendix Fig S4A). The top-30 downregulated and top-30 upregulated genes are shown in Appendix Tables S3 and S4, respectively. Furthermore, we validated selected genes from these lists with a special focus on genes with indicated roles in neuronal development, function and survival by RT-qPCR (Appendix Fig S4B and C).

Performing a custom analysis on splicing efficiency (described in Materials and Methods), we detected more than 400 introns that are differentially spliced in the FUS-depleted cells. Whereas only a very small fraction of major introns were found to be differentially spliced in the FUS-depleted cells, more than 30% of the minor introns that are expressed in SH-SY5Y cells exhibit differential splicing (Fig 4C). In fact, minor introns are highly overrepresented among the differentially spliced introns compared to the numbers one would expect if major intron splicing and minor intron splicing were affected to the same extent by FUS depletion (Fig 4D). The finding that splicing of minor introns is much stronger affected than the splicing of major introns by the absence of FUS is in line with the preference of FUS towards the minor spliceosome constituent U11 snRNP and the GO analysis of the spectrometry results. While the gene-level analysis showed both up- and downregulation of minor intron-containing genes in response to FUS depletion, the majority of the minor introns detected by our differential splicing analysis are spliced more efficiently, which would suggest that FUS mainly functions as a splicing inhibitor. However, the underrepresentation of transcripts whose splicing is promoted by FUS can be attributed to their rapid degradation by the nuclear exosome that was shown to specifically degrade mRNAs with retained minor introns (Niemela *et al*, 2014). Additionally, mRNAs with a retained intron that escape decay by the nuclear exosome and are exported to the cytoplasm very likely will harbour premature termination codons and hence be degraded by the nonsense-mediated mRNA decay (NMD) pathway (Schweingruber *et al*, 2013). Hence, the actual number of affected minor introns might be even higher than estimated by our splicing efficiency analysis, because aberrant mRNAs with retained minor introns would most likely undergo a rapid degradation and therefore not be easily detectable in the FUS-depleted SH-SY5Y cells.

To examine whether these effects of FUS on splicing of minor introns can also be observed in mice, we re-analysed published mRNA-seq data from mouse brain (Lagier-Tourenne *et al*, 2012). Corroborating the results from the human neuroblastoma cells, we found that the splicing of minor introns tends to be more affected by FUS depletion than the splicing of major introns also in mouse brain (Appendix Fig S4D). The abundance of many minor intron-containing mRNAs was altered upon FUS depletion and overall mRNAs harbouring at least one minor intron were more affected by

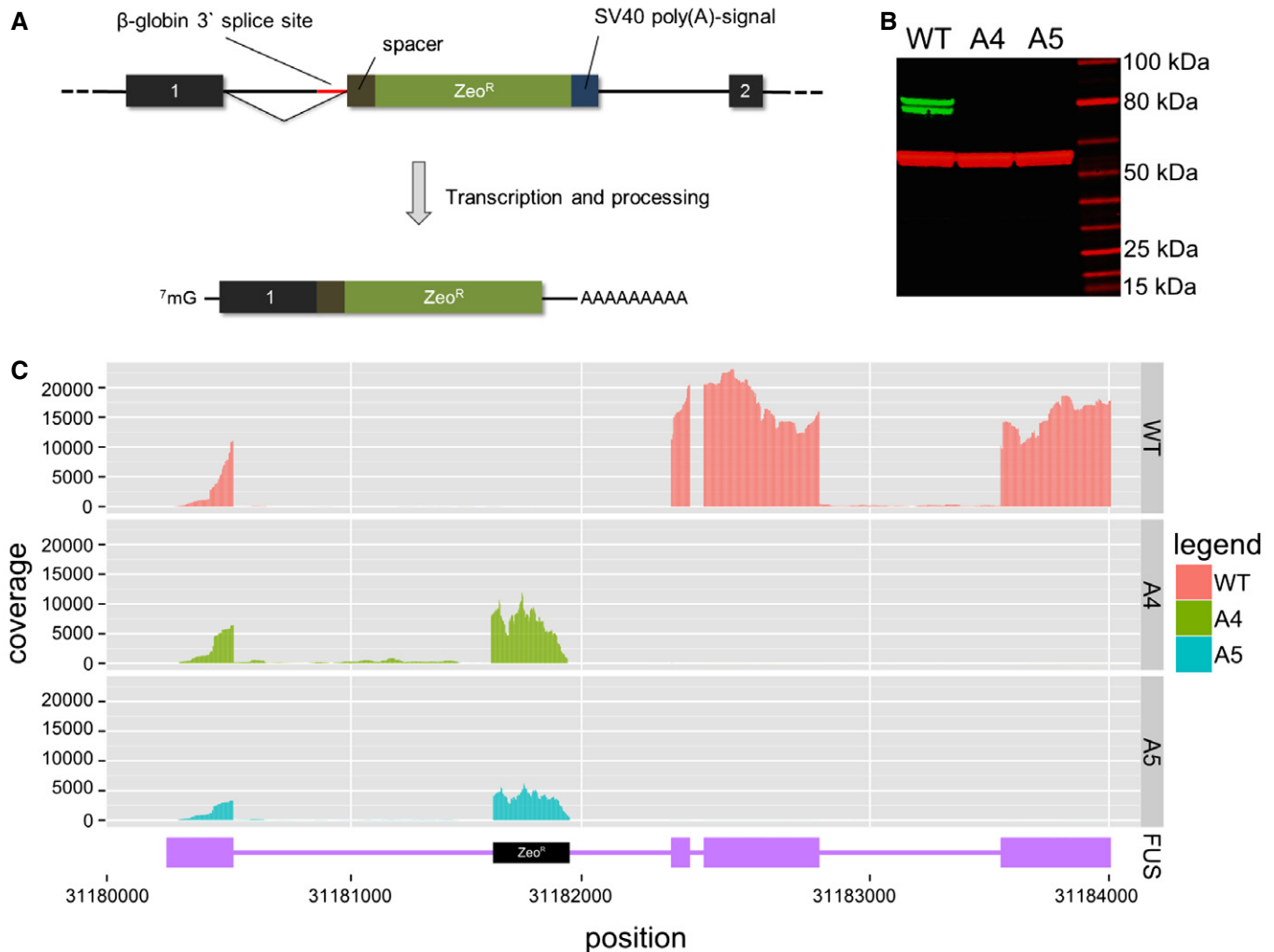


**Figure 3. FUS knockout in SH-SY5Y neuroblastoma cells.**

- A** Scheme of the FUS-knockout strategy in SH-SY5Y neuroblastoma cells. The first intron of the FUS gene was targeted with CRISPR/Cas9 to introduce a DNA cassette consisting of a chimeric intron with a strong 3' splice site (red line), a spacer sequence (olive-green box), the coding sequence of the Sh ble gene, which confers Zeocin resistance (Zeo<sup>R</sup>, green box), and the SV40 polyadenylation signal (blue box). Upon transcription from the FUS promoter, the first exon of FUS is spliced in frame to this Zeo<sup>R</sup>-encoding exon and the SV40 polyadenylation signal causes the premature polyadenylation of the FUS mRNA.
- B** Western blot confirming the absence of FUS in the two selected clones. Extracts from wild-type (wt) and FUS-knockout SH-SY5Y cells (clones A4 and A5) were subjected to SDS-PAGE, transferred to a nitrocellulose membrane and FUS (green) and tyrosine tubulin (red; loading control) were detected using respective primary and secondary antibodies.
- C** Reads from the mRNA-seq of the SH-SY5Y neuroblastoma cells mapped to the FUS gene. The first four exons and the intervening introns of the FUS gene are depicted in purple (boxes indicate exons, and thin lines indicate introns; for better visualization, intron lengths are reduced by a factor of five compared to exons). The mapped reads to this locus are shown on a log<sub>10</sub> scale for the wild-type cells (red), FUS KO clone A4 (green) and FUS KO clone A5 (blue). In the two FUS KO clones, hardly any reads are detected downstream of the introduced Zeo<sup>R</sup> cassette.

Source data are available online for this figure.

FUS depletion than mRNAs containing exclusively major introns even in mouse brain (Appendix Fig S4E).

Given the strong effect of FUS on minor intron splicing, we next tested whether FUS preferentially associates with minor intron-containing RNA. We performed RNA immunoprecipitations (RIPs) with endogenous FUS from SH-SY5Y cells and observed that the proportion of minor intron-containing genes was significantly higher among the RNAs enriched in our FUS-RIP compared to the mRNAs that were not significantly enriched or those that were even

underrepresented in the FUS-RIP, indicating a higher affinity of FUS for minor introns relative to major introns (Appendix Fig S4F).

#### FUS acts like a classical hnRNP on minor intron-containing reporter genes

To investigate whether the observed splicing effects on minor introns are a direct consequence of the FUS depletion, we used the well-studied p120-derived minor intron minigene version in which

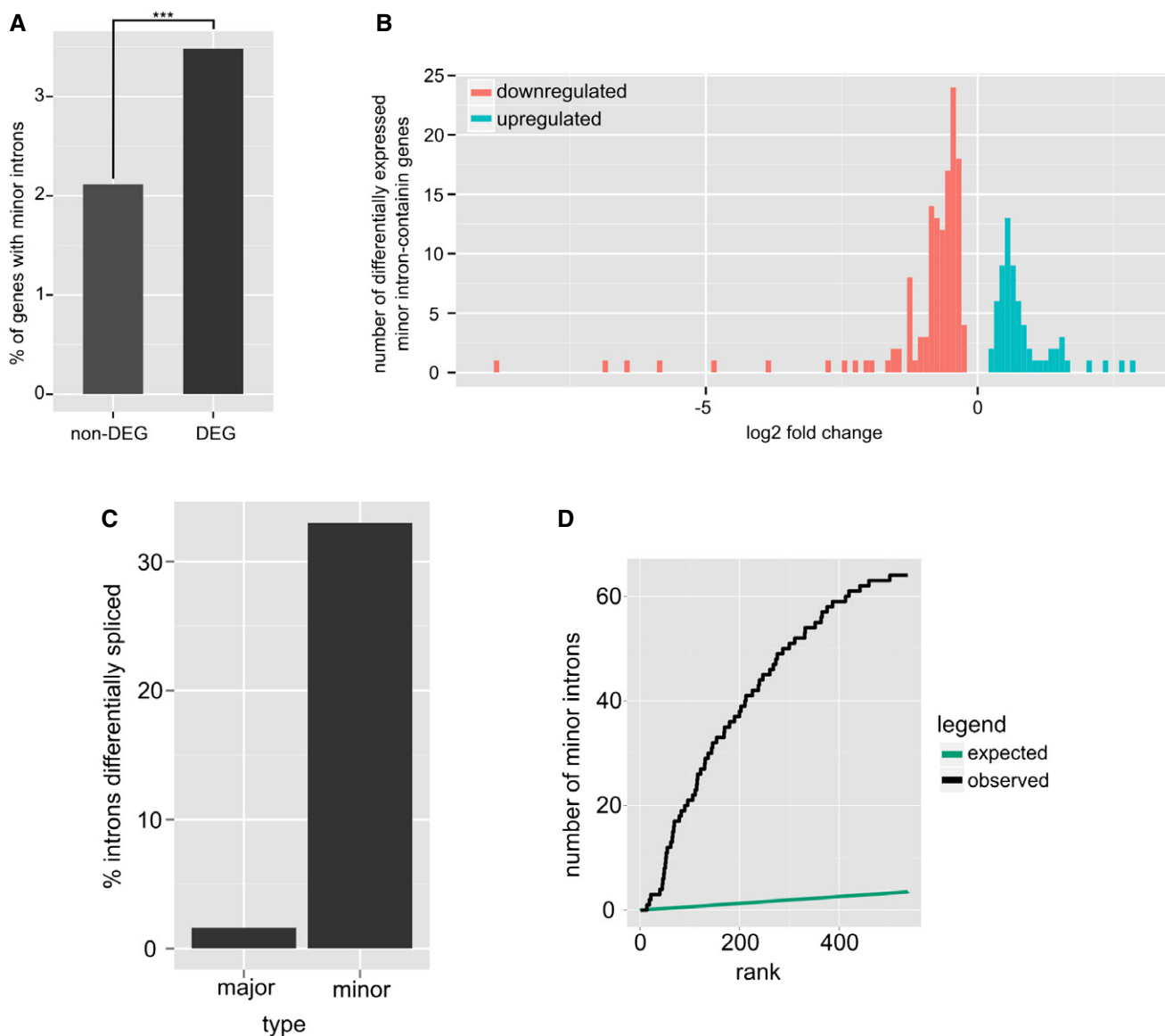


**Figure 4. FUS depletion deregulates splicing of minor introns.**

From four biological replicates of FUS KO SH-SY5Y clones A4 and A5 as well as wild-type cells, poly(A)-selected cDNAs were prepared and sequenced on a Illumina HiSeq3000 machine and the data were analysed as described in Materials and Methods.

- A** Analysis of RNA-seq results focusing on the transcripts of genes containing at least one minor intron. Genes were divided into two categories depending on whether they were differentially expressed upon FUS KD (DEG) or whether their expression was not affected (non-DEG). The percentage of genes with at least one minor intron is depicted for both categories. Compared to the non-DEG, the % of minor intron-containing genes is significantly enriched in the DEG. Effect size: 1.65,  $P$ -value:  $3.49e-10$ .
- B** Histogram of differentially expressed minor intron-containing genes. Genes are grouped according to the level of differential expression. Approximately two-thirds of the affected genes are downregulated in the absence of FUS.
- C** Bar plot showing the percentage of differentially spliced introns among all expressed introns. Major and minor introns are displayed separately. More than 30% of minor introns are differentially spliced under FUS knockout, whereas only a small subset of the major introns are affected.
- D** The cumulative plot shows the abundance of minor splice sites among the most differentially expressed splice sites in the RNA-seq data from the FUS KO SH-SY5Y cells. The most differentially expressed sites (ranked from left to right) are depicted on the x-axis, while the y-axis shows the number of minor splice sites among them. The black line represents the distribution observed in the RNA-seq data. This distribution was compared to what would be expected if minor and major splice sites were equally affected by the FUS knockout. This hypothetical distribution (shown in green) was computed with a hypergeometric function. This analysis reveals a high enrichment for minor splice sites, indicating that the usage of minor splice sites is more often altered upon FUS KO relative to the usage of major splice sites.

the hnRNP H-binding G-rich tracts that are required to recruit the minor spliceosome were replaced by MS2 binding sites (p120-MS2bs) (McNally *et al*, 2006; Fig 5A). The pre-mRNA with the MS2

binding sites is spliced very inefficiently unless a factor promoting the recruitment of the minor spliceosome (e.g. hnRNP H) is tethered to the MS2 binding sites by expressing it as a fusion protein with the

MS2 coat protein (MS2CP) (McNally *et al*, 2006). We co-expressed FLAG-tagged FUS without the MS2CP moiety and MS2-EGFP as negative controls as well as MS2-hnRNP H and MS2-FUS together with p120-MS2bs minigene in HeLa cells, confirmed their expression by Western blot (Fig 5B) and analysed their effect on the splicing of this minigene by RT-qPCR to determine the ratio of spliced to unspliced reporter mRNA as a measure for splicing efficiency. Neither the tethering of MS2-EGFP nor the expression of FLAG-tagged FUS without the MS2CP moiety led to a significant increase in splicing, whereas tethering of MS2-hnRNP H or MS2-FUS led to a more than 35- and 55-fold increase in the ratio of spliced to unspliced mRNA, respectively (Fig 5C), indicating that FUS plays a direct role in recruiting the U11/U12 di-snRNP to minor introns.

Using the tethering system, we next set out to identify the parts of FUS required for promoting splicing. We created a series of truncation and deletion mutants of FUS, all comprising an N-terminal MS2CP fusion and the C-terminal FUS NLS to assure nuclear localization (Fig 5D). After co-expression of the MS2CP fusion proteins with the p120-MS2bs, we analysed their expression by Western blot (Fig 5E) and tested their ability to promote the splicing of the minor intron (Fig 5F). Compared to the splicing activity obtained by tethering of full-length FUS, deletion of the first 284 amino acids (the QGSY-rich and RGG1 domains) almost completely abrogated the capacity of FUS to promote splicing of the p120 intron. A series of C-terminal truncations identified that the first 165 amino acids (the QGSY-rich region) were sufficient for promoting p120 intron removal. Importantly, the FET binding motif (FETbm), which mediates homo- and heterodimer formation between the FET family members (Thomsen *et al*, 2013), is dispensable for the splicing activity conveyed by the 1–165 FUS fragment, indicating that the attraction of the minor spliceosome does not depend on an interaction with the other FET family members.

Besides promoting splicing, the mRNA-seq data indicated that FUS also inhibits the splicing efficiency of several minor introns. Therefore, we wondered whether FUS might function like a classical hnRNP: binding of an hnRNP within an intron usually enhances splicing, while binding within an exon inhibits splicing of the adjacent intron or leads to exon skipping. For major introns, it was already reported that tethering of hnRNPs into introns can promote their splicing and that tethering of the same hnRNPs into the corresponding exons can inhibit the splicing of these introns (Erkelenz *et al*, 2013). To test this position-dependent splicing function

concept on minor introns, we generated a version of the p120 minigene in which we inserted the MS2 binding sites into the exon 5' of the intron (p120-MS2bs-ex7) (Fig 5G). Indeed, tethering of FUS into the exon of the p120 reporter strongly suppressed its splicing (Fig 5H and I). As for the promotion of splicing, the first 165 amino acids of FUS lacking the FETbm were also sufficient for splicing suppression. Taken together, these data show that FUS can directly promote or suppress splicing of minor introns depending on its binding position on the pre-mRNA.

### Minor intron-containing genes are deregulated in FUS-depleted cells

Since we observed that many minor intron-containing genes are downregulated in the FUS KO SH-SY5Y cells (Fig 4B and Appendix Fig S4A), we assessed whether the inefficient splicing of the minor introns could account for the observed downregulation of these genes. To address this question, we took advantage of three already established minor intron-containing minigenes, namely the p120-derived minor intron minigene and the SCN4A and mouse SCN8A minor intron-derived minigenes (McNally *et al*, 2006; Howell *et al*, 2007; Fig 6A). Noteworthy, SCN8A and p120 are expressed in SH-SY5Y cells and both of them were downregulated in the FUS KO cells (Appendix Fig S4A). Moreover, the SCN4A and SCN8A genes are involved in several neurological and neuromuscular disorders and are required for the initiation and/or propagation of action potentials in the skeletal muscle and spinal motor neurons, respectively (Porter *et al*, 1996; Eijkelkamp *et al*, 2012).

We transfected HeLa cells with these minigenes along with knockdown-inducing pSUPuro plasmids expressing either a short hairpin (sh)RNA targeting the FUS mRNA (FUS KD) or an shRNA with a scrambled sequence as control knockdown (Ctr KD). Three days later, we analysed the FUS protein levels by Western blotting (Fig 6B). We observed that FUS depletion reduced the splicing efficiency of the minor intron in all three reporter genes (Fig 6C). Importantly, this effect was rescued by co-transfection of an expression plasmid encoding an RNAi-resistant version of FUS. We also validated whether the endogenous SCN4A mRNA is affected by FUS depletion. Since SCN4A is almost exclusively expressed in the skeletal muscle (Trimmer *et al*, 1989), we used the rhabdomyosarcoma cell line RH-30 for this experiment. Indeed, siRNA-induced

#### Figure 5. Tethering of FUS promotes splicing of minor introns.

- A Schematic representation of the p120-MS2bs minigene construct, which contains two MS2-binding sites in its minor intron instead of the hnRNP H-binding motifs.
- B Western blot confirming the expression of MS2CP fusion proteins. Extracts from mock-transfected HeLa cells, FUS-FLAG and MS2CP fusion protein-expressing cells were subjected to SDS-PAGE and Western blot followed by the detection of exogenous proteins by anti-FLAG (green, lanes 1–2) and anti-MS2 (green, lanes 3–5) antibodies, respectively. Tyrosine tubulin (red) served as a loading control.
- C The ratio of spliced to unspliced p120-MS2bs RNA was determined by RT-qPCR from cells expressing the indicated MS2 fusion proteins. Average values and standard deviations of seven biological replicates are shown.
- D Schematic representation of MS2-FUS deletion constructs used in the tethered splicing assay shown in (E and F).
- E Western blot confirming the expression of MS2CP fusion proteins as in (B). The MS2 fusion proteins were detected by anti-MS2 antibodies (green) and tyrosine tubulin (red) served as a loading control.
- F The ratio of spliced to unspliced p120-MS2bs RNA was measured as in (C). Average values and standard deviations of at least three biological replicates are shown.
- G Schematic representation of the p120-MS2bs-ex7 minigene construct, which contains two MS2-binding sites in exon 7.
- H Western blot confirming the expression of MS2CP fusion proteins as in (E).
- I The ratio of spliced to unspliced p120-MS2bs-ex7 was measured as in (C). Average values and standard deviations of three biological replicates are shown.

Source data are available online for this figure.

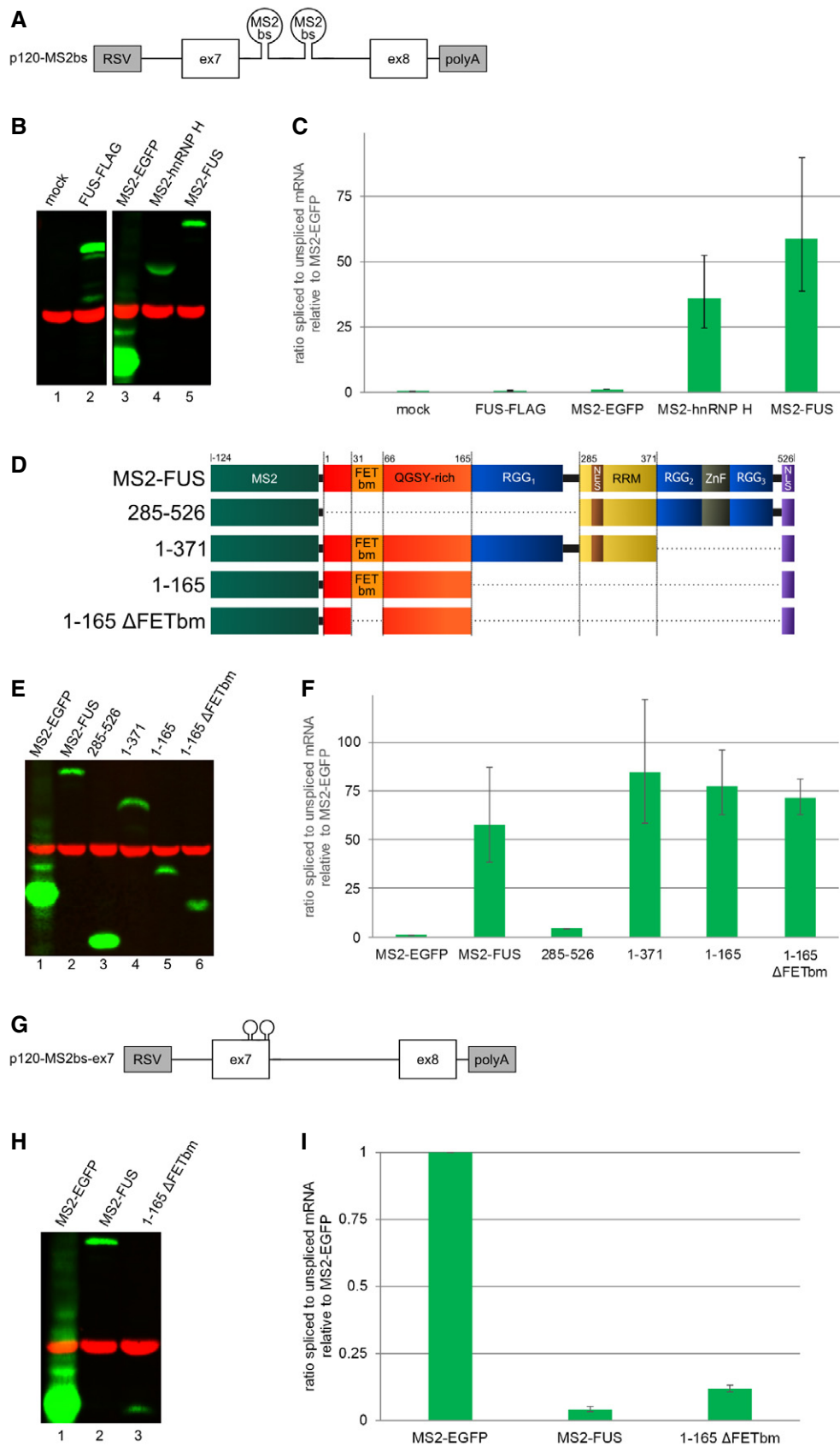
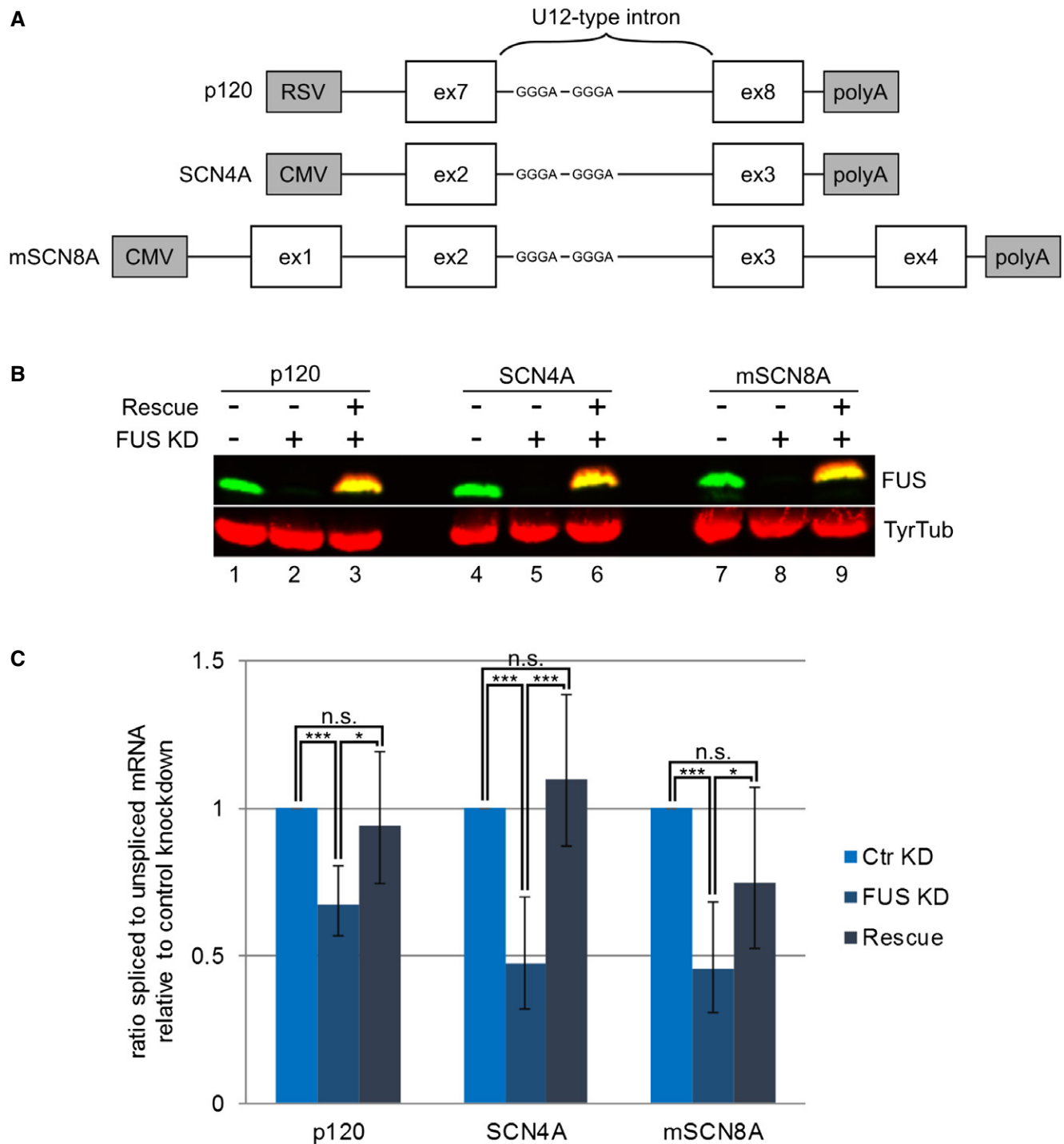


Figure 5.



**Figure 6. FUS promotes splicing of minor intron-containing reporter genes.**

A Schematic representation of the minor intron-containing p120, SCN4A and mSCN8A minigenes and their promoters (rouv sarcoma virus [RSV] or cytomegalovirus [CMV]). HnRNP H-binding sites are depicted as GGGG.

B Western blot analysis of FUS levels under control knockdown (lanes 1, 4, 7), FUS knockdown (FUS KD; lanes 2, 5, 8) and FUS rescue (lanes 3, 6, 9). HeLa cell extracts were subjected to SDS-PAGE and Western blotting with anti-FUS antibodies (green) and anti-FLAG (red, upper part). The yellow signal in the upper part is due to the overlay of the red and the green channels. Tyrosine tubulin was detected as a loading control (red, lower part).

C RT-qPCR results indicating the ratio of spliced to unspliced RNA from the indicated minigenes under control knockdown (Ctr KD), FUS KD and FUS KD followed by a rescue with an RNAi-resistant cDNA expression construct (Rescue). Average values and standard deviations are shown of nine biological replicates for p120 and SCN4A (five including the rescue condition) and of eight biological replicates for mSCN8A (all including the rescue). \* $P < 0.05$  and \*\*\* $P < 0.001$ .

Source data are available online for this figure.

knockdown of FUS decreased SCN4A mRNA in RH-30 cells (Appendix Fig S5).

Since all the aforementioned minigenes contain predicted hnRNP H-binding sites, we further tested whether hnRNP H is a prerequisite for FUS function in minor intron splicing. In contrast to mouse SCN8A, the human SCN8A minor intron lacks predicted hnRNP H-binding sites, but contains instead hnRNP M binding sites close to the 5' splice site (Appendix Fig S6A and B). Nonetheless, FUS depletion also led to a significant reduction in the splicing efficiency of the human SCN8A minigene (Appendix Fig S6C and D). Interestingly, hnRNP M is one of our high-confidence FUS interactors (Appendix Table S1), and its interaction with FUS was recently reported (Marko *et al.*, 2014). This indicates that FUS might promote splicing of both hnRNP H- and hnRNP M-bound minor introns and possibly of introns bound by additional hnRNPs.

### An ALS-associated FUS mutation inhibits minor intron splicing and causes mislocalization of U11 and U12 snRNA to the cytoplasm

The very C-terminus of FUS harbours the NLS (Fig 7A) and many ALS-associated mutations have been shown to affect the interaction of the NLS with transportin, leading to a reduced concentration of FUS in the nucleus (Dormann *et al.*, 2010). The tethering-dependent splicing assay provided an opportunity to test whether the reduction in nuclear FUS concentration caused by the NLS-inactivating ALS-associated P525L mutation affects FUS's function in splicing. To this end, we co-expressed MS2-tagged FUS-P525L with the p120-MS2bs reporter gene. As expected, immunofluorescence confirmed that the FUS-P525L localized mainly to the cytoplasm with only a small amount of protein still residing in the nucleus, in contrast to the almost exclusive nuclear localization of wild-type FUS (Fig 7B). When expressed at similar levels, MS2-FUS-P525L exhibited significantly less splicing activity than wild-type MS2-FUS in the tethering assay (Fig 7C and D). The splicing activity of the P525L mutant could be restored by appending an SV40 NLS to MS2-FUS-P525L (Fig 7A), which also restored the nuclear localization of the protein (Fig 7B), demonstrating that the reduced nuclear level of FUS P525L was responsible for its failure to efficiently promote p120 intron splicing.

Since recent studies showed that the U1 and U2 snRNAs mislocalize upon the expression of ALS-associated FUS mutants that

accumulate in the cytoplasm (Germino *et al.*, 2013; Yu *et al.*, 2015), we wondered whether the minor spliceosome components U11 and U12 snRNAs might be affected similarly. Indeed, we could confirm by fluorescence *in situ* hybridization combined with immunofluorescence that upon the expression of MS2-FUS-P525L but not MS2-FUS-wild type, the U11 (Fig 7E) and U12 snRNA (Fig 7F) colocalized with the mutant FUS to cytoplasmic granules, while their abundance appears to be reduced in the nucleus. Moreover, the first 165 amino acids of FUS, which are sufficient to promote or repress splicing in the tethered splicing assays, were also sufficient to mislocalize U11 as well as U12 snRNA into the cytoplasm (Appendix Fig S7A and B). This suggests that the ALS-associated mutations in the NLS of FUS contribute to the disease not only by the lack of nuclear FUS needed for correct splicing of a subset of FUS-regulated minor introns, but additionally also by trapping U11 and U12 snRNA in the cytoplasm and therewith affecting the splicing of all minor introns.

## Discussion

Collectively, our results demonstrate that FUS regulates the splicing of minor introns. FUS associates with several hnRNPs and with the U12-type spliceosomal complex (Figs 1 and 2, Appendix Figs S1 and S2 and Appendix Table S1). Knockout of FUS leads to a severe deregulation of minor intron splicing and its depletion inhibits splicing of minor intron-containing minigenes (Figs 4 and 6 and Appendix Fig S6A). Furthermore, we show that FUS directly promotes or represses splicing of minor introns when tethered into an intron or a preceding exon, respectively, thereby acting as a classical hnRNP (Fig 5). The analysis of our high-throughput sequencing data sets revealed that i) minor intron-containing mRNAs are more affected by FUS depletion and ii) minor intron-containing mRNAs are bound more often by FUS compared to major introns (Fig 4 and Appendix Fig S4). The ALS-associated FUS mutant P525L fails to promote minor intron splicing due to its mislocalization to the cytoplasm, which in turn traps U11 and U12 snRNAs in cytoplasmic FUS aggregates, causing a clearance of these factors from the nucleus (Fig 7). Our findings are graphically summarized in Fig 8 and are in agreement with the proposed two-hit model for FUS-associated ALS (Dormann *et al.*, 2010). Under normal circumstances, most FUS resides in the nucleus and regulates the splicing of minor introns, possibly in conjunction with other hnRNPs. In the

### Figure 7. FUS P525L is deficient in promoting minor intron splicing and mislocalizes U11 and U12 snRNA in the cytoplasm.

- A Schematic representation of the MS2-FUS (wild type), MS2-FUS P525L and MS2-FUS P525L fused to an SV40 NLS constructs used in the tethered splicing assay.
- B Immunofluorescence on HeLa cells showing the localization of wild-type, P525L- and P525L-SV40-NLS MS2-FUS fusion proteins. MS2 fusion proteins were visualized with anti-MS2 antibodies and the nucleus was stained with DAPI. Scale bar = 10  $\mu$ m.
- C Western blot documenting comparable expression levels of the MS2-FUS constructs. Cell extracts were subjected to SDS-PAGE and Western blotting followed by the detection of the MS2 fusion proteins by anti-MS2 antibodies (green). Tyrosine tubulin (red) served as a loading control.
- D RT-qPCR results depicting the ratio of spliced to unspliced p120-MS2bs reporter RNA from cells co-expressing the indicated MS2 fusion proteins. Average values and standard deviations of three biological replicates are shown, **\*\*P < 0.01**.
- E Combined FISH and immunofluorescence on HeLa cells transiently expressing MS2-FUS (upper panel) or MS2-FUS P525L (lower panel). MS2 fusion proteins were visualized with anti-MS2 antibodies (red), U11 snRNA with 6-FAM azide-labelled RNA complementary to the full-length snRNA (green) and nuclei were stained with DAPI. Scale bar = 10  $\mu$ m.
- F As in (E) but with a probe detecting U12 snRNA (green).

Source data are available online for this figure.

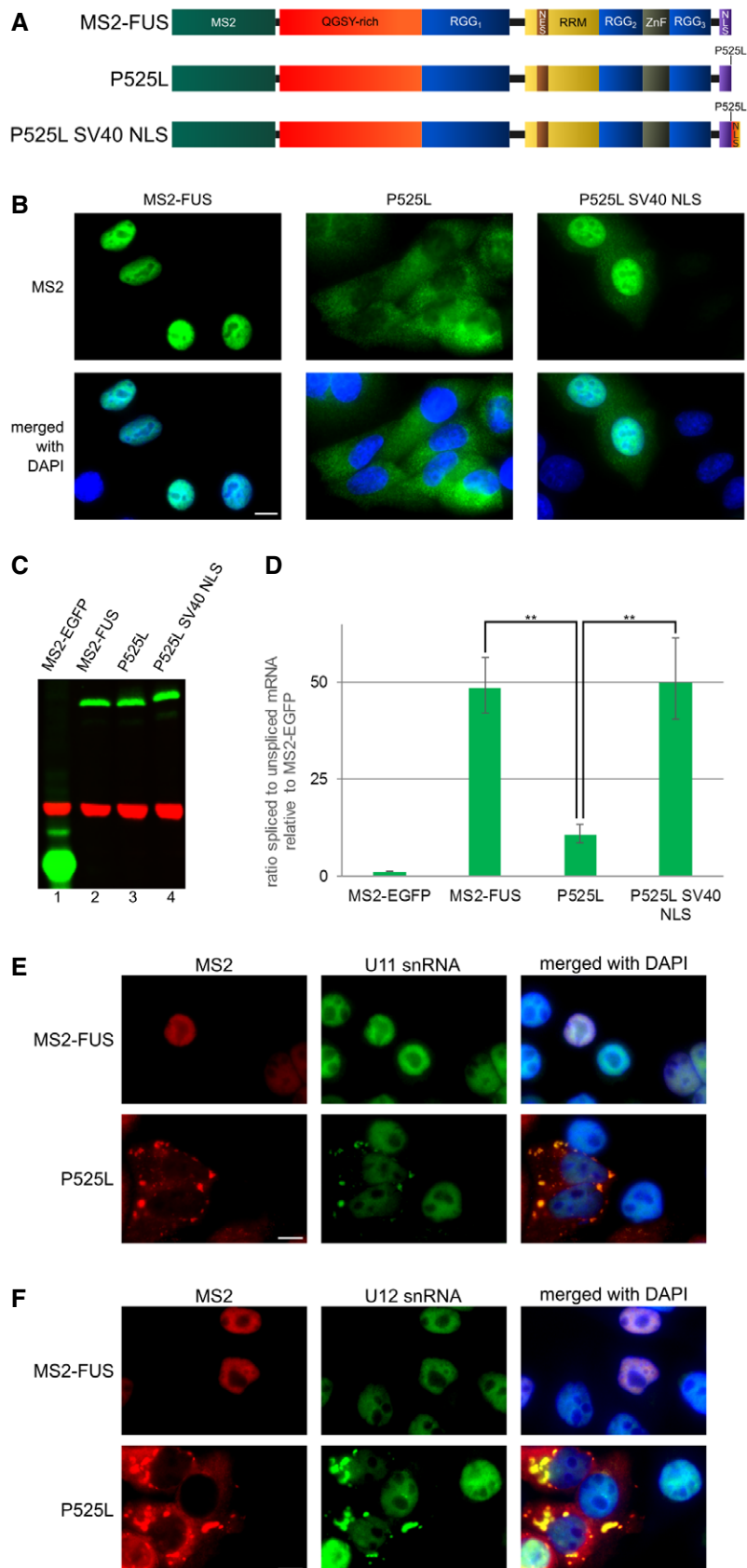
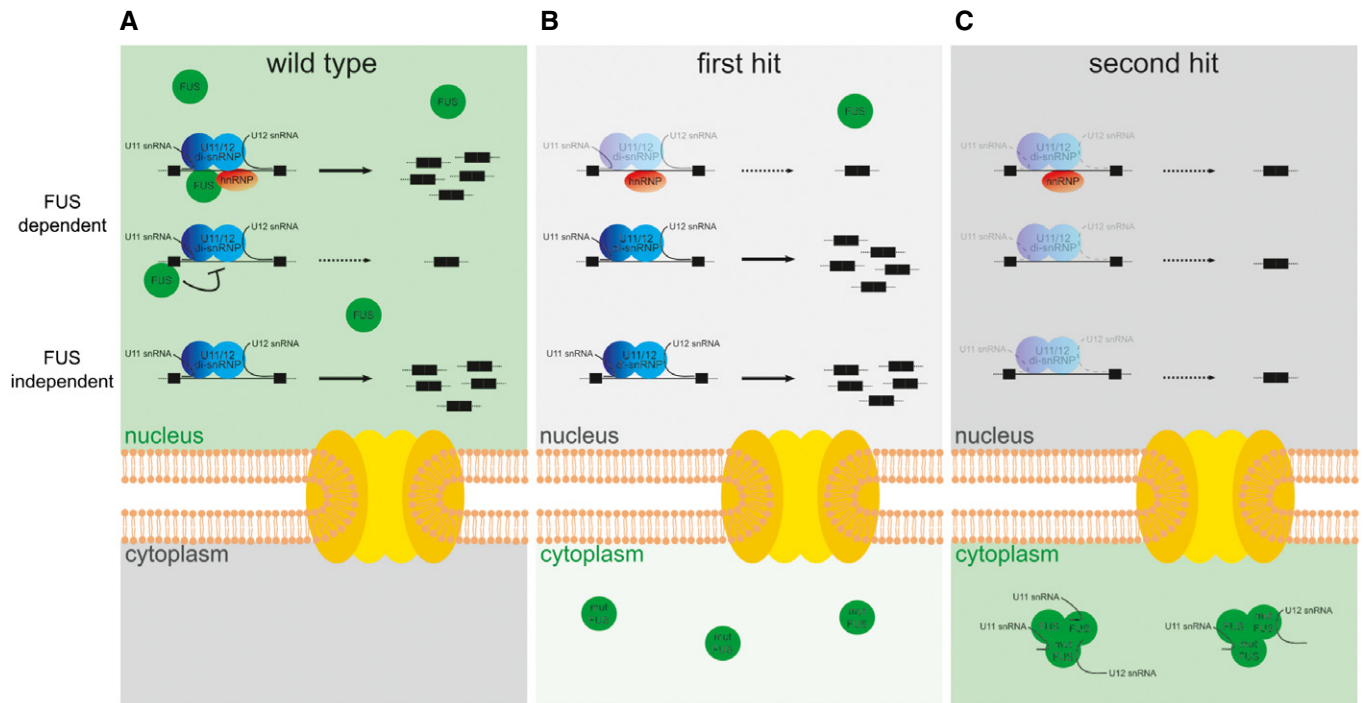


Figure 7.



**Figure 8. Model depicting the consequences of ALS-associated NLS-inactivating FUS mutations on splicing.**

- A Wild-type FUS localizes to the nucleus and binds, presumably in conjunction with other hnRNPs, its direct pre-mRNA targets to regulate splicing of minor introns.
- B Mutations inactivating the NLS of FUS (= first hit) reduce the nuclear abundance of FUS, resulting in deregulated splicing of the direct targets (i.e. FUS-dependent minor introns), whereas other minor intron-containing mRNAs are not yet affected.
- C Over time, due to repeated stress (= second hit), mutant FUS leads to the formation of cytoplasmic aggregates, which further reduces the amount of FUS in the nucleus due to trapping of wild-type FUS in these aggregates along with U11 and U12 snRNAs. This affects now not only the splicing of FUS-dependent minor introns, but leads to a general inhibition of minor intron-containing mRNAs due to the reduction in nuclear U11 and U12 snRNAs.

context of ALS-associated FUS NLS mutations (first hit), the mutant FUS re-localizes to the cytoplasm and its nuclear levels are reduced, which deregulates splicing of its direct targets. Once cytoplasmic FUS-containing aggregates form due to the repeated stress (second hit), increasing amounts of U11 and U12 snRNAs become trapped in these aggregates, leading to a shortage of minor spliceosome components in the nucleus and ultimately to a general inhibition of minor intron splicing.

Recent studies showed that U1 and U2 snRNAs also mislocalize to FUS-containing cytoplasmic aggregates upon the expression of ALS-associated FUS mutants (Gerbino *et al*, 2013; Yu *et al*, 2015). However, taking into account that U1 and U2 snRNAs are about threefold more abundant than FUS, whereas U11 and U12 snRNAs are > 30-fold less abundant than FUS (Lerner & Steitz, 1979; Montzka & Steitz, 1988; Singh *et al*, 2015), the minor spliceosome is much more at risk of being functionally affected by the sequestration U11 and U12 snRNAs into cytoplasmic FUS aggregates than the major spliceosome by sequestration of U1 and U2 snRNAs, respectively.

#### Evidence for cooperation of hnRNPs and FUS in binding mRNA

So far, several FUS-CLIP studies have been conducted (Hoell *et al*, 2011; Lagier-Tourenne *et al*, 2012; Rogelj *et al*, 2012; Nakaya *et al*, 2013; Zhou *et al*, 2013; Masuda *et al*, 2015), but no common

sequence motifs could be identified. It was recently shown that FUS binds RNA *in vitro* in the higher nM range, but without apparent preference for a specific sequence or structure (Wang *et al*, 2015), begging the question how FUS gains specificity *in vivo*. Since a quarter of our identified high-confidence FUS interactors are hnRNPs (Appendix Table S1), one reason for the lack of a common consensus motif could be that FUS gains specificity through the interaction with its hnRNP partners and that different hnRNPs guide FUS to different binding elements. Such a cooperative binding mode with different hnRNPs would obscure the identification of individual specific binding motifs and could explain the failure to detect common consensus motifs among the different CLIP experiments. Consistent with such a cooperative mode of RNA binding, we observed that tethered hnRNP H requires FUS for the efficient splicing promotion, whereas tethered FUS still efficiently promoted the splicing in the absence of hnRNP H (Appendix Fig S8). This suggests that hnRNP H helps FUS to bind to the minor intron in order to have FUS available for minor spliceosome recruitment. This mode of action might also apply to other hnRNPs, for example hnRNP M.

#### Implications of FUS's role in minor intron splicing

The minor spliceosome is essential for development (Otake *et al*, 2002; Baumgartner *et al*, 2015), and dysfunctional minor splicing

has been associated with several developmental and neurological disorders. In humans, mutations in the U4atac snRNA lead to the developmental disorder Taby-Linder syndrome (TALS), which is characterized by the growth retardation as well as central nervous system malformations (Pierce & Morse, 2012; Jafarifar *et al*, 2014). In spinal muscular atrophy (SMA), the levels of the U11/U12 di-snRNP and the minor tri-snRNP are reduced (Gabanelia *et al*, 2007; Zhang *et al*, 2008; Boulisfane *et al*, 2011), which affects the proper processing of minor intron-containing mRNAs coding for a protein required for motor circuit function (Lotti *et al*, 2012). Recent studies have shown that also in TDP-43-associated ALS, the integrity of the minor spliceosome is affected (Ishihara *et al*, 2013; Tsuiji *et al*, 2013). Together with our findings, this suggests that ALS, SMA, as well as neurological defects observed in other diseases such as TALS, converge in that they all exhibit the defects in minor spliceosome function.

Strikingly, apart from the two most-affected minor intron-containing genes that encode for PPP2R2C and ACTL6B, which are required for the promotion of neurogenesis and dendritic development, respectively (Strack, 2002; Wu *et al*, 2007), a high amount of voltage-gated calcium as well as sodium channels are affected by the FUS depletion (Appendix Tables S3 and S4, Appendix Fig S4B and C). Intriguingly, two of the voltage-gated sodium channels that are directly regulated by FUS are required for action potential transmission and for functional spinal motor units. The first is SCN8A, which initiates and transmits action potentials in central neurons and their myelinated axons (Catterall *et al*, 2005). The loss of SCN8A expression results in skeletal muscle atrophy due to the loss of functional innervation (Duchen & Stefani, 1971; Angaut-Petit *et al*, 1982; Kohrman *et al*, 1996). Additionally, SCN8A is essential for post-natal maturation of spinal motor units, but not oculomotor units (Porter *et al*, 1996). Intriguingly, the oculomotor neurons are spared from the observed neurodegeneration in ALS (Haenggeli & Kato, 2002). The second is SCN4A, which initiates and transmits the action potential in skeletal muscles. While for SOD1-associated ALS, the role of muscle cells in the pathomechanism remains controversial (Ilieva *et al*, 2009), our data provide evidence that hampered expression of genes with minor introns not only in motor neurons but also in muscle cells could contribute to the disease.

It remains to be elucidated whether minor intron splicing defects are a main cause or the last nudge over the edge for motor neuron death. While further investigations using patient material and *in vivo* models will be required to dissect the exact role of minor intron splicing in neurodegeneration, minor spliceosome defects appear to emerge as a common characteristic of several neurological disorders.

## Materials and Methods

Detailed descriptions of oligonucleotides, plasmids, antibodies and of additional methods can be found in the Appendix.

### Cell culture and plasmid transfections

HeLa, 293T and SH-SY5Y cells were cultivated in Dulbecco's modified Eagle's medium (DMEM) supplemented with 10% foetal calf serum (FCS), penicillin (100 IU/ml) and streptomycin (100 µg/ml)

(DMEM + / +) and grown at 37°C and 5% CO<sub>2</sub>. Plasmid DNA transfections were performed with Dreamfect, Dogtor (OZ Biosciences) and Eugene HD (Promega), whereas siRNA transfections were performed using Lipofectamine 2000 according to the manufacturer's instructions.

### Immunoprecipitations for mass spectrometric analysis

Total extracts from 293T cells transfected with pcDNA3-FUS-GSG15-FLAG or pcDNA3-EBFP-GSG15-FLAG were prepared either in the absence (RNase free) or in the presence of 0.2 mg/ml RNase A (RNase treated). The lysate was cleared by centrifugation (15 min at 16,100 g at 4°C) and the supernatant was incubated with anti-FLAG™ M2 affinity gel. The affinity gel was suspended in 1 ml NET-2 (50 mM Tris-HCl pH 7.5, 150 mM NaCl, 0.05% Triton X-100) and washed five times by subsequent suspension and centrifugation steps. For the high salt interactors (750 mM), the precipitates from RNase A-treated extracts were washed three times with NET-2 supplemented with NaCl to a final concentration of 750 mM. Finally, immunoprecipitated protein complexes were eluted with FLAG peptide, subjected to SDS-PAGE and analysed by mass spectrometry.

### Sample preparation and mass spectrometric analysis

For in-gel tryptic digestion, the lanes of interest were excised from the Coomassie-stained gels and subdivided into 10 gel slices. Disulfide bonds were reduced with 10 mM dithiothreitol for 30 min at 56°C, alkylated with 55 mM iodoacetamide for 20 min at room temperature in the dark and digested overnight at 37°C with bovine trypsin (Sigma Aldrich) as previously described (Shevchenko *et al*, 2006). The resulting peptide mixture was desalted and concentrated using the C18 StageTips procedure as previously described (Rappsilber *et al*, 2007). Mass spectrometry analysis was performed by nano liquid chromatography coupled to tandem MS (nLC-ESI-MS/MS) using a LTQ-Orbitrap mass spectrometer (Thermo Scientific) as follows: 5 µl of purified peptide mixture was injected into the chromatographic system (EasyLC, Proxeon Biosystems) and the peptides were separated on a 25-cm fused silica capillary column (75 µm inner diameter and 360 µm outer diameter, Proxeon Biosystems) filled with Reprosil-Pur C18 3 µm resin (Dr. Maisch GmbH, Ammerbuch-Entringen, Germany) using a pressurized packing bomb. Peptides were eluted with a 95-min gradient from 7 to 70% of buffer B (80% ACN, 0.5% acetic acid) at a flow rate of 200 nl/min. The LC system was connected to the LTQ-Orbitrap equipped with a nano electrospray ion source. Full-scan mass spectra were acquired in the LTQ-Orbitrap mass spectrometer in the mass range m/z 350–1750 Da and with resolution set to 60,000. The lock-mass option was used to internally calibrate mass spectra for most accurate mass measurements. The 10 most intense doubly and multiply charged ions were automatically selected and fragmented in the ion trap with a CID set to 35%.

### Peptides and proteins identification by database searching

Raw data files were analysed using the peptide search engine Andromeda, which is integrated into the MaxQuant software environment (version 1.5.2.8; Cox *et al*, 2011), with the following

parameters: uniprot\_cp\_hum\_2015\_01 as protein database, oxidation (M), acetyl (protein N-term), as variable modifications, carbamidomethyl (C) as fixed modifications, peptide false discovery rate (FDR) 0.01, maximum peptide posterior error probability (PEP) 1, protein FDR 0.01, minimum peptides 2, at least 1 unique, minimum length peptide 6 amino acids. Two biological replicates were performed for each immunoprecipitation and mass spectrometry analysis. Only proteins identified in both replicates were selected for further analysis.

### Gene ontology (GO) enrichment analysis

Gene ontology terms enrichment analysis was performed with the PANTHER (Protein ANalysis THrough Evolutionary Relationships) classification system (Mi *et al.*, 2013), using the gene names of the identified proteins as queries for the statistical overrepresentation test and the most updated *Homo sapiens* genes annotations as reference set. The electronically inferred annotations were excluded and only the overrepresented categories with a *P*-value < 0.05 are shown in the graphs.

### RNA immunoprecipitation (RIP) from HeLa nuclear extracts

About 180  $\mu$ l of protein G Dynabeads was coupled to 40  $\mu$ g of FUS antibody in TBS–0.05% NP-40 for 2 h head over tail at 4°C, followed by two washes with TBS–NP-40 to remove uncoupled antibodies. To each sample, fresh TBS–NP-40 and 60  $\mu$ l of HeLa nuclear extract (IPRACELL, Mons, Belgium) were added and incubated head over tail for 1.5 h at 4°C. After five washes with TBS–NP-40, the beads were resuspended in 1 ml TRIZOL and RNA was isolated according to the manufacturer's instructions. As input, 60  $\mu$ l of nuclear extract was directly added to 1 ml of TRIZOL; 2  $\mu$ g of RNA were reverse-transcribed at 37°C in 50  $\mu$ l containing 1 $\times$  small RNA RT buffer (10 mM Tris, pH 8, 75 mM potassium, 10 mM dithiothreitol, 70 mM magnesium chloride, 0.8 mM anchored universal RT primer), 2 U/ $\mu$ l of RiboLock (Fermentas), 10 mM dNTPs, 2.5 mM rATP supplemented with 5 U of *Escherichia coli* poly(A) polymerase (New England Biolabs) and 1  $\mu$ l of AffinityScript reverse transcriptase (Agilent). Reactions were heat-inactivated for 10 min at 85°C. Reverse-transcribed material corresponding to 18 ng of RNA was amplified with MESA GREEN qPCR Master Mix Plus for SYBR (Eurogentec) and the appropriate primers (600 nM each) in a total volume of 20  $\mu$ l using the Rotorgene 6000 (Corbett). Primer sequences are listed in Appendix Table S2.

### Biotinylated antisense oligonucleotide pull-down

About 200  $\mu$ l of magnetic streptavidin Dynabeads slurry (MyOne T1, Life Technologies) was washed three times with PBS and blocked for 30 min at 4°C in blocking buffer (250  $\mu$ g/ml tRNA, 250  $\mu$ g/ml glycogen, 250  $\mu$ g/ml BSA in PBS); 400  $\mu$ l of buffer D+/+ (20 mM HEPES pH 7.9, 100 mM KCl, 20% glycerol, 0.25 mM EDTA, 0.5 mM DTT, 1 $\times$  protease inhibitor, 1 $\times$  phosphatase inhibitor, 0.01% NP-40) was supplemented with 100  $\mu$ l of HeLa nuclear extract (HNE, Ipracell) and 200 pmol biotinylated U11 antisense oligonucleotide (ACGACAGAAGCCUUUU-Bio-Bio-Bio, Microsynth) (Will *et al.*, 1999). As a negative control, the antisense oligonucleotide was omitted. The oligonucleotides were hybridized for 45 min

head over tail at 30°C. The reactions were cleared by centrifugation (16,100 g for 5 min), and the supernatants were transferred to new Eppendorf tubes; 100  $\mu$ l of blocked streptavidin beads was added to each supernatant and incubated for 45 min at 4°C head over tail. Subsequently, the beads were washed five times with 1 ml of buffer D+/+ supplemented with 0.05% NP-40. With the last wash, the beads were transferred to new Eppendorf tubes, wash buffer was removed and the beads were resuspended in 50  $\mu$ l of 2 $\times$  LDS-loading buffer, boiled for 10 min at 70°C and loaded on a 4–12% NuPAGE gel.

### U12-dependent splicing under FUS-knockdown conditions

About 2.5  $\times$  10<sup>5</sup> HeLa cells were seeded per well of a 6-well plate in DMEM<sup>+/+</sup> (day 0). On day 1, the cells were co-transfected with 100 ng reporter construct and 500 ng pSUPuro-FUS or pSUPuro-scrambled, respectively, using Dogtor. For functional rescue experiments, 800 ng of pcDNA6F-FUS-RNAiR WT was co-transfected, in addition. On day 2, the cells were split into a T25 flask in DMEM<sup>+/+</sup> containing 2  $\mu$ g/ml puromycin (Santa Cruz). On day 3, the medium was replaced by DMEM<sup>+/+</sup> without puromycin; 6–8 h later, the cells were harvested and the relative mRNA levels were quantified by RT–qPCR (described in the Appendix).

### Tethered splicing assay

About 2.5  $\times$  10<sup>5</sup> HeLa cells were seeded per well of a 6-well plate in DMEM<sup>+/+</sup> (day 0). On day 1, the cells were co-transfected using Dogtor, 300–800 ng plasmid coding for the MS2-fusion protein (DNA amount depending on the expression of respective construct) and 100–400 ng reporter construct (400 ng only if co-transfected with plasmids encoding MS2-FUS P525L or MS2-FUS P525L NLS; to compare MS2-FUS with the two P525L variants, also pcDNA3.1(+)-MS2-FUS was co-transfected with 400 ng reporter plasmid). Cells were split into a T25 flask on day 2 and harvested on day 3, and the relative mRNA levels were quantified by RT–qPCR.

To investigate tethered splicing under FUS KD conditions, HeLa cells were transfected with additional 500 ng pSUPuro-FUS or pSUPuro-scrambled, respectively, on day 1. On day 2, the cells were split into a T25 flask in DMEM<sup>+/+</sup> containing 2  $\mu$ g/ml puromycin (Santa Cruz). On day 3, the medium was replaced by DMEM<sup>+/+</sup> containing no puromycin, and 6–8 h later, the cells were harvested.

To investigate tethered splicing under hnRNP H KD conditions, HeLa cells were co-transfected with 100 ng reporter construct, 500 ng plasmid coding for MS2-EGFP or MS2-FUS, respectively, and 100 pmol siRNA targeting hnRNP H or control siRNA (Appendix Table S2) using Lipofectamine 2000 on day 1 and a second time on day 3 of the experiment. On day 4, the cells were split into a T25 flask and harvested on day 5.

### RIP from SH-SY5Y cells coupled to high-throughput sequencing

Three times 1  $\times$  10<sup>7</sup> SH-SY5Y cells were lysed in a total of 5.1 ml hypotonic gentle lysis buffer supplemented with 2 $\times$  protease inhibitor (Pierce), 1 $\times$  PhosStop phosphatase inhibitor (Roche), 4 U/ml Turbo DNase and 0.2 U/ $\mu$ l SUPERasin. After 10-min incubation on ice, NaCl was adjusted to 150 mM, followed by another 5-min incubation on ice. The lysate was centrifuged at 16,100 g for 15 min at

4°C to remove insoluble material; 1.5 ml of the supernatant was recovered, spiked with 75 µl of SH-SY5Y extract from the cells expressing U6-AmdS-4xSON stemloop and incubated with Dynabeads coupled to 50 µg of rabbit anti-FUS antibody (for the input sample, 300 µl supernatant plus 15 µl of spike extract were directly added to 1 ml TRI reagent). Immune complexes were allowed to form for 1.5 h at 4°C rotating head over tail. After incubation, the beads were washed five times with NET-2 (50 mM Tris pH 7.4, 150 mM NaCl, 0.05% Triton X-100) supplemented with 0.01 U/µl SUPERasin. With the sixth wash, the beads were transferred to fresh tubes, the supernatant was removed and 1 ml of TRI reagent was added to the beads. RNA was isolated according to the TRI reagent protocol (Life Technologies), except that precipitation was carried out with 2 volumes of 2-propanol, the addition of 2 µl of glycogen, precipitation overnight at -20°C, precipitation by centrifugation at 16,100 g for 1 h and two subsequent washes with 85 and 80% EtOH, respectively. The pellets were then dried in the speed vac and resuspended in MilliQ-H<sub>2</sub>O. Quality and quantity of the isolated RNA were assessed with an Agilent 2100 Bioanalyzer (Agilent Technologies) and Qubit 2.0 Fluorometer (Life Technologies). Approximately 250 ng of high-quality RNA was used for strand-specific paired-end RNA library preparation (TruSeq stranded mRNA sample preparation guide Part #15031047 Rev.D, Illumina). Total mRNA libraries were multiplexed and sequenced in a single lane on the Illumina HiSeq2000 platform using 2 × 100 bp paired-end sequencing cycles. The Illumina BCL output files with base calls and qualities were converted into FASTQ file format and demultiplexed with the Casava software (v1.8.2; Illumina).

### Bioinformatics analysis

Sequences produced from the RNA-seq experiment of FUS-RIP were mapped with the software TopHat v2.0.9 (Trapnell *et al*, 2009) to the human genome (GRCh37) with standard options. The mapping process was aided by the use of a gtf transcriptome file from Ensembl as scaffold (GRCh37.75). The mapped reads were then sorted with the program samtools (v0.9.19). The counting was performed with the Python package HTSeq (Anders *et al*, 2015), with the following options: -r name -s reverse -a 0 -m union, using the previously mentioned transcriptome file. The differential expression analysis was performed with DESeq2 (Love *et al*, 2014). The size factors used in the normalization step of this algorithm were computed on the 1,000 most highly expressed genes. Information about minor introns was collected from U12DB (Alioto, 2007). The same pipeline was applied to the data obtained by the sequencing of the FUS KO clones, with the following differences: the reference human genome and transcriptome file were taken from a more recent release (GRCh38.81). Additionally, the adjusted *P*-values resulting from the gene-level analysis of each individual clone, compared to WT, were analysed with the sum of *P*-values method, in order to produce a synthetic significance score.

The splicing analysis was performed with a custom program. For every known and novel splice junction observed in the data, we collected the number of reads across the junction and inside the intron. Every location that contained an additional splice donor or acceptor site was removed from the analysis. Every thus determined intron was then investigated for an equal coverage. Furthermore, a strict filter on the number of reads was applied, removing sites with

low expression and high variability. The software DESeq2 was finally employed to compute the significance of intron retention between WT and KO conditions. The program was run on the intron counts table, applying the normalization of the splice counts, thus analysing the unspliced/spliced ratio of every junction in a robust statistical set-up. The code is available as a Python package at the following address: <https://github.com/Martombo/SpliceRatio>.

Sequences obtained from Lagier-Tourenne *et al* (2012) were pre-processed with the program Trimmomatic (Bolger *et al*, 2014) and mapped with TopHat to the mouse genome (GRCm38) guiding the process with a transcriptome file from Ensembl (GRCm38.78). The counting was performed with the Python package HTSeq and the differential expression analysis with DESeq2 as described above.

### Fluorescence *in situ* hybridization (FISH) in combination with immunofluorescence

HeLa cells transfected either with wild-type MS2-FUS or with MS2-FUS P525L expression plasmids were seeded in 8-chamber slides, fixed with 4% paraformaldehyde and permeabilized with 70% EtOH. The exogenous FUS protein was stained with rabbit anti-MS2 antibody and a species-specific DyLight 594-coupled secondary antibody. Thereafter, the cells were post-fixed and U11 and U12 snRNA were detected by hybridization with 6-FAM-labelled antisense RNA probes. After subsequent washes to remove unbound probes, the slides were mounted with Vectashield containing DAPI and the images were acquired.

### Data availability

#### Primary data

The mass spectrometry data from this publication have been submitted to the Peptide Atlas repository database and assigned the accession number PASS00730.

The high-throughput sequencing data of the RNA-IP of FUS and of the FUS KO clones from this publication have been submitted to the GEO SRA database (Edgar *et al*, 2002) and assigned the identifier GSE71812.

#### Referenced data

RNA-seq data of FUS KD in mouse brains, published by Lagier-Tourenne *et al* (2012), were retrieved from the GEO SRA database, under the accession ID GSE40653.

**Expanded View** for this article is available online.

### Acknowledgements

We would like to thank Lisa and Mark McNally (Medical College of Wisconsin) and Miriam Meisler (University of Michigan) for the generous gift of plasmids, Ramesh Pillai (EMBL Grenoble) for providing FUS antibodies, Douglas Black (Howard Hughes Medical Institute, UCLA) for providing hnRNP H antibodies, Irina Banzola and Beat Schäfer (University of Zürich) for providing the RH-30 cells and Daniel Schümperli for providing SH-SY5Y cells. We also thank Cord Drögemüller, Tosso Leeb and Michèle Ackermann of the NGS platform (University of Bern) for technical advice and library preparation and Nicole Kleinschmidt and Karin Schranz for excellent technical support. We gratefully acknowledge the support of the NOMIS Foundation, the NCCR RNA and Disease funded by the Swiss National Science Foundation, the Holcim Stiftung

zur Förderung der wissenschaftlichen Fortbildung, the Swiss Life Jubiläumstiftung, the Fondation Dufloateau and the Canton Bern.

### Author contributions

SR, OM and MDR conceived and designed the experiments. SR, JS, GF, MC, DJ and MDR performed the experiments and data interpretation. GF, SCL, CS, AB, RB and SMLB contributed to experimental design and data interpretation. SR, OM and MDR wrote the manuscript with the contributions of JS, GF, MC, CS and SMLB.

### Conflict of interest

The authors declare that they have no conflict of interest.

## References

- Alioto TS (2007) U12DB: a database of orthologous U12-type spliceosomal introns. *Nucleic Acids Res* 35: D110–D115
- Aman P, Panagopoulos I, Lassen C, Fioretos T, Mencinger M, Toresson H, Hoglund M, Forster A, Rabbitts TH, Ron D, Mandahl N, Mitelman F (1996) Expression patterns of the human sarcoma-associated genes FUS and EWS and the genomic structure of FUS. *Genomics* 37: 1–8
- Anders S, Pyl PT, Huber W (2015) HTSeq—a Python framework to work with high-throughput sequencing data. *Bioinformatics* 31: 166–169
- Angaut-Petit D, McArdle JJ, Mallart A, Bournaud R, Pincon-Raymond M, Rieger F (1982) Electrophysiological and morphological studies of a motor nerve in ‘motor endplate disease’ of the mouse. *Proc Biol Sci* 215: 117–125
- Baumgartner M, Lemoine C, Al Seesi S, Karunakaran DK, Sturrock N, Bandy AR, Kilcollins AM, Mandoiu I, Kanadia RN (2015) Minor splicing snRNAs are enriched in the developing mouse CNS and are crucial for survival of differentiating retinal neurons. *Dev Neurobiol* 75: 895–907
- Behzadnia N, Golas MM, Hartmuth K, Sander B, Kastner B, Deckert J, Dube P, Will CL, Urlaub H, Stark H, Luhrmann R (2007) Composition and three-dimensional EM structure of double affinity-purified, human prespliceosomal A complexes. *EMBO J* 26: 1737–1748
- Bentmann E, Haass C, Dormann D (2013) Stress granules in neurodegeneration—lessons learnt from TAR DNA binding protein of 43 kDa and fused in sarcoma. *FEBS J* 280: 4348–4370
- Bolger AM, Lohse M, Usadel B (2014) Trimmomatic: a flexible trimmer for Illumina sequence data. *Bioinformatics* 30: 2114–2120
- Boulisfane N, Choleza M, Rage F, Neel H, Soret J, Bordonne R (2011) Impaired minor tri-snRNP assembly generates differential splicing defects of U12-type introns in lymphoblasts derived from a type I SMA patient. *Hum Mol Genet* 20: 641–648
- Catterall WA, Goldin AL, Waxman SG (2005) International Union of Pharmacology. XLVII. Nomenclature and structure-function relationships of voltage-gated sodium channels. *Pharmacol Rev* 57: 397–409
- Cox J, Neuhauser N, Michalski A, Scheltema RA, Olsen JV, Mann M (2011) Andromeda: a peptide search engine integrated into the MaxQuant environment. *J Proteome Res* 10: 1794–1805
- Deckert J, Hartmuth K, Boehringer D, Behzadnia N, Will CL, Kastner B, Stark H, Urlaub H, Luhrmann R (2006) Protein composition and electron microscopy structure of affinity-purified human spliceosomal B complexes isolated under physiological conditions. *Mol Cell Biol* 26: 5528–5543
- DeJesus-Hernandez M, Kocerha J, Finch N, Crook R, Baker M, Desaro P, Johnston A, Rutherford N, Wojtas A, Kennelly K, Wszolek ZK, Graff-Radford N, Boylan K, Rademakers R (2010) De novo truncating FUS gene mutation as a cause of sporadic amyotrophic lateral sclerosis. *Hum Mutat* 31: E1377–E1389
- Dormann D, Rodde R, Edbauer D, Bentmann E, Fischer I, Hruscha A, Than ME, Mackenzie IRA, Capell A, Schmid B, Neumann M, Haass C (2010) ALS-associated fused in sarcoma (FUS) mutations disrupt Transportin-mediated nuclear import. *EMBO J* 29: 2841–2857
- Duan R, Sharma S, Xia Q, Garber K, Jin P (2014) Towards understanding RNA-mediated neurological disorders. *J Genet Genomics* 41: 473–484
- Duchen LW, Stefani E (1971) Electrophysiological studies of neuromuscular transmission in hereditary ‘motor end-plate disease’ of the mouse. *J Physiol* 212: 535–548
- Edgar R, Domrachev M, Lash AE (2002) Gene expression Omnibus: NCBI gene expression and hybridization array data repository. *Nucleic Acids Res* 30: 207–210
- Eijkelkamp N, Linley JE, Baker MD, Minett MS, Cregg R, Werdehausen R, Rugiero F, Wood JN (2012) Neurological perspectives on voltage-gated sodium channels. *Brain* 135: 2585–2612
- Erkelenz S, Mueller WF, Evans MS, Busch A, Schoneweis K, Hertel KJ, Schaal H (2013) Position-dependent splicing activation and repression by SR and hnRNP proteins rely on common mechanisms. *RNA* 19: 96–102
- Gabanella F, Butchbach ME, Saieva L, Carissimi C, Burghes AH, Pellizzoni L (2007) Ribonucleoprotein assembly defects correlate with spinal muscular atrophy severity and preferentially affect a subset of spliceosomal snRNPs. *PLoS One* 2: e921
- Gerbino V, Carri MT, Cozzolino M, Achsel T (2013) Mislocalised FUS mutants stall spliceosomal snRNPs in the cytoplasm. *Neurobiol Dis* 55: 120–128
- Hackl W, Fischer U, Luhrmann R (1994) A 69-kD protein that associates reversibly with the Sm core domain of several spliceosomal snRNP species. *J Cell Biol* 124: 261–272
- Haenggeli C, Kato AC (2002) Differential vulnerability of cranial motoneurons in mouse models with motor neuron degeneration. *Neurosci Lett* 335: 39–43
- Hartmuth K, Urlaub H, Vornlocher HP, Will CL, Gentzel M, Wilm M, Luhrmann R (2002) Protein composition of human prespliceosomes isolated by a tobramycin affinity-selection method. *Proc Natl Acad Sci USA* 99: 16719–16724
- Hoell JI, Larsson E, Runge S, Nusbaum JD, Duggimpudi S, Farazi TA, Hafner M, Borkhardt A, Sander C, Tuschl T (2011) RNA targets of wild-type and mutant FET family proteins. *Nat Struct Mol Biol* 18: 1428–1431
- Howell VM, Jones JM, Bergren SK, Li L, Billi AC, Avenarius MR, Meisler MH (2007) Evidence for a direct role of the disease modifier SCNM1 in splicing. *Hum Mol Genet* 16: 2506–2516
- Iko Y, Kodama TS, Kasai N, Oyama T, Morita EH, Muto T, Okumura M, Fujii R, Takumi T, Tate S, Morikawa K (2004) Domain architectures and characterization of an RNA-binding protein, TLS. *J Biol Chem* 279: 44834–44840
- Ilieva H, Polymenidou M, Cleveland DW (2009) Non-cell autonomous toxicity in neurodegenerative disorders: ALS and beyond. *J Cell Biol* 187: 761–772
- Ishihara T, Ariizumi Y, Shiga A, Kato T, Tan CF, Sato T, Miki Y, Yokoo M, Fujino T, Koyama A, Yokoseki A, Nishizawa M, Kakita A, Takahashi H, Onodera O (2013) Decreased number of Gemini of coiled bodies and U12 snRNA level in amyotrophic lateral sclerosis. *Hum Mol Genet* 22: 4136–4147
- Jafarifar F, Dietrich RC, Hiznay JM, Padgett RA (2014) Biochemical defects in minor spliceosome function in the developmental disorder MOPD I. *RNA* 20: 1078–1089
- Jurkat-Rott K, Holzherr B, Fauler M, Lehmann-Horn F (2010) Sodium channelopathies of skeletal muscle result from gain or loss of function. *Pflugers Arch* 460: 239–248

- Kohrman DC, Harris JB, Meisler MH (1996) Mutation detection in the med and medJ alleles of the sodium channel Scn8a. Unusual splicing due to a minor class AT-AC intron. *J Biol Chem* 271: 17576–17581
- Kwiatkowski TJ, Bosco DA, LeClerc AL, Tamrazian E, Vanderburg CR, Russ C, Davis A, Gilchrist J, Kasarskis EJ, Munsat T, Valdmanis P, Rouleau GA, Hosler BA, Cortelli P, de Jong PJ, Yoshinaga Y, Haines JL, Pericak-Vance MA, Yan J, Ticozzi N et al (2009) Mutations in the FUS/TLS gene on chromosome 16 cause familial amyotrophic lateral sclerosis. *Science* 323: 1205–1208
- Lagier-Tourenne C, Cleveland DW (2009) Rethinking ALS: the FUS about TDP-43. *Cell* 136: 1001–1004
- Lagier-Tourenne C, Polymenidou M, Hutt KR, Vu AQ, Baughn M, Huelga SC, Clutario KM, Ling SC, Liang TY, Mazur C, Wancewicz E, Kim AS, Watt A, Freier S, Hicks GG, Donohue JP, Shiue L, Bennett CF, Ravits J, Cleveland DW et al (2012) Divergent roles of ALS-linked proteins FUS/TLS and TDP-43 intersect in processing long pre-mRNAs. *Nat Neurosci* 15: 1488–1497
- Lerner MR, Steitz JA (1979) Antibodies to small nuclear RNAs complexed with proteins are produced by patients with systemic lupus erythematosus. *Proc Natl Acad Sci USA* 76: 5495–5499
- Li X, Decker M, Westendorf JJ (2010) TETHERed to Runx: novel binding partners for runx factors. *Blood Cells Mol Dis* 45: 82–85
- Lotti F, Imlach Wendy L, Saieva L, Beck Erin S, Le Hao T, Li Darrick K, Jiao W, Mentis George Z, Beattie Christine E, McCabe Brian D, Pellizzoni L (2012) An SMN-dependent U12 splicing event essential for motor circuit function. *Cell* 151: 440–454
- Love MI, Huber W, Anders S (2014) Moderated estimation of fold change and dispersion for RNA-seq data with DESeq2. *Genome Biol* 15: 550
- Marko M, Leichter M, Patrino-Georgoula M, Guialis A (2014) Selective interactions of hnRNP M isoforms with the TET proteins TAF15 and TLS/FUS. *Mol Biol Rep* 41: 2687–2695
- Masuda A, Takeda J, Okuno T, Okamoto T, Ohkawara B, Ito M, Ishigaki S, Sobue G, Ohno K (2015) Position-specific binding of FUS to nascent RNA regulates mRNA length. *Genes Dev* 29: 1045–1057
- McNally LM, Yee L, McNally MT (2006) Heterogeneous nuclear ribonucleoprotein H is required for optimal U11 small nuclear ribonucleoprotein binding to a retroviral RNA-processing control element: implications for U12-dependent RNA splicing. *J Biol Chem* 281: 2478–2488
- Meissner M, Lopato S, Gotzmann J, Sauer mann G, Barta A (2003) Proto-oncoprotein TLS/FUS is associated to the nuclear matrix and complexed with splicing factors PTB, SRm160, and SR proteins. *Exp Cell Res* 283: 184–195
- Mi H, Muruganujan A, Casagrande JT, Thomas PD (2013) Large-scale gene function analysis with the PANTHER classification system. *Nat Protoc* 8: 1551–1566
- Montzka KA, Steitz JA (1988) Additional low-abundance human small nuclear ribonucleoproteins: U11, U12, etc. *Proc Natl Acad Sci USA* 85: 8885–8889
- Nakaya T, Alexiou P, Maragkakis M, Chang A, Mourelatos Z (2013) FUS regulates genes coding for RNA-binding proteins in neurons by binding to their highly conserved introns. *RNA* 19: 498–509
- Niemela EH, Oghabian A, Staals RH, Greco D, Puijij GJ, Frilander MJ (2014) Global analysis of the nuclear processing of transcripts with unspliced U12-type introns by the exosome. *Nucleic Acids Res* 42: 7358–7369
- Otake LR, Scamborova P, Hashimoto C, Steitz JA (2002) The divergent U12-type spliceosome is required for pre-mRNA splicing and is essential for development in *Drosophila*. *Mol Cell* 9: 439–446
- Pierce MJ, Morse RP (2012) The neurologic findings in Taybi-Linder syndrome (MOPD I/III): case report and review of the literature. *Am J Med Genet A* 158A: 606–610
- Porter JD, Goldstein LA, Kasarskis EJ, Brueckner JK, Spear BT (1996) The neuronal voltage-gated sodium channel, Scn8a, is essential for postnatal maturation of spinal, but not oculomotor, motor units. *Exp Neurol* 139: 328–334
- Rappsilber J, Mann M, Ishihama Y (2007) Protocol for micro-purification, enrichment, pre-fractionation and storage of peptides for proteomics using StageTips. *Nat Protoc* 2: 1896–1906
- Rappsilber J, Ryder U, Lamond AI, Mann M (2002) Large-scale proteomic analysis of the human spliceosome. *Genome Res* 12: 1231–1245
- Rogelj B, Easton LE, Bogu GK, Stanton LW, Rot G, Curk T, Zupan B, Sugimoto Y, Modic M, Haberman N, Tollervey J, Fujii R, Takumi T, Shaw CE, Ule J (2012) Widespread binding of FUS along nascent RNA regulates alternative splicing in the brain. *Sci Rep* 2: 603
- Schwartz JC, Ebmeier CC, Podell ER, Heimiller J, Taatjes DJ, Cech TR (2012) FUS binds the CTD of RNA polymerase II and regulates its phosphorylation at Ser2. *Genes Dev* 26: 2690–2695
- Schweiggruber C, Rufener SC, Zund D, Yamashita A, Muhlemann O (2013) Nonsense-mediated mRNA decay - mechanisms of substrate mRNA recognition and degradation in mammalian cells. *Biochim Biophys Acta* 1829: 612–623
- Shevchenko A, Tomas H, Havlis J, Olsen JV, Mann M (2006) In-gel digestion for mass spectrometric characterization of proteins and proteomes. *Nat Protoc* 1: 2856–2860
- Singh G, Pratt G, Yeo GW, Moore MJ (2015) The clothes make the mRNA: past and present trends in mRNP fashion. *Annu Rev Biochem* 84: 325–354
- Strack S (2002) Overexpression of the protein phosphatase 2A regulatory subunit Bgamma promotes neuronal differentiation by activating the MAP kinase (MAPK) cascade. *J Biol Chem* 277: 41525–41532
- Sun S, Ling SC, Qiu J, Albuquerque CP, Zhou Y, Tokunaga S, Li H, Qiu H, Bui A, Yeo GW, Huang EJ, Eggen K, Zhou H, Fu XD, Lagier-Tourenne C, Cleveland DW (2015) ALS-causative mutations in FUS/TLS confer gain and loss of function by altered association with SMN and U1-snRNP. *Nat Commun* 6: 6171
- Tan AY, Manley JL (2010) TLS inhibits RNA polymerase III transcription. *Mol Cell Biol* 30: 186–196
- Thomsen C, Grundevik P, Elias P, Ståhlberg A, Åman P (2013) A conserved N-terminal motif is required for complex formation between FUS, EWSR1, TAF15 and their oncogenic fusion proteins. *FASEB J* 27: 4965–4974
- Trapnell C, Pachter L, Salzberg SL (2009) TopHat: discovering splice junctions with RNA-Seq. *Bioinformatics* 25: 1105–1111
- Trimmer JS, Cooperman SS, Tomiko SA, Zhou JY, Crean SM, Boyle MB, Kallen RG, Sheng ZH, Barchi RL, Sigworth FJ, Goodman RH, Agnew WS, Mandel G (1989) Primary structure and functional expression of a mammalian skeletal muscle sodium channel. *Neuron* 3: 33–49
- Tsujii H, Iguchi Y, Furuya A, Kataoka A, Hatsuta H, Atsuta N, Tanaka F, Hashizume Y, Akatsu H, Murayama S, Sobue G, Yamanaka K (2013) Spliceosome integrity is defective in the motor neuron diseases ALS and SMA. *EMBO Mol Med* 5: 221–234
- Uranishi H, Tetsuka T, Yamashita M, Asamitsu K, Shimizu M, Itoh M, Okamoto T (2001) Involvement of the pro-oncoprotein TLS (translocated in liposarcoma) in nuclear factor-kappa B p65-mediated transcription as a coactivator. *J Biol Chem* 276: 13395–13401
- Vance C, Rogelj B, Hortobagyi T, De Vos KJ, Nishimura AL, Sreedharan J, Hu X, Smith B, Ruddy D, Wright P, Ganesalingam J, Williams KL, Tripathi V, Al-Saraj S, Al-Chalabi A, Leigh PN, Blair IP, Nicholson G, de Belleroche J, Gallo JM et al (2009) Mutations in FUS, an RNA processing protein, cause familial amyotrophic lateral sclerosis type 6. *Science* 323: 1208–1211

- Wang WY, Pan L, Su SC, Quinn EJ, Sasaki M, Jimenez JC, Mackenzie IR, Huang EJ, Tsai LH (2013) Interaction of FUS and HDAC1 regulates DNA damage response and repair in neurons. *Nat Neurosci* 16: 1383–1391
- Wang X, Schwartz JC, Cech TR (2015) Nucleic acid-binding specificity of human FUS protein. *Nucleic Acids Res* 43: 7535–7543
- Will CL, Luhrmann R (2011) Spliceosome structure and function. *Cold Spring Harb Perspect Biol* 3: a003707
- Will CL, Schneider C, Reed R, Luhrmann R (1999) Identification of both shared and distinct proteins in the major and minor spliceosomes. *Science* 284: 2003–2005
- Wu JI, Lessard J, Olave IA, Qiu Z, Ghosh A, Graef IA, Crabtree GR (2007) Regulation of dendritic development by neuron-specific chromatin remodeling complexes. *Neuron* 56: 94–108
- Yamazaki T, Chen S, Yu Y, Yan B, Haertlein TC, Carrasco MA, Tapia JC, Zhai B, Das R, Lalancette-Hebert M, Sharma A, Chandran S, Sullivan G, Nishimura AL, Shaw CE, Gygi SP, Shneider NA, Maniatis T, Reed R (2012) FUS-SMN protein interactions link the motor neuron diseases ALS and SMA. *Cell Rep* 2: 799–806
- Yu Y, Chi B, Xia W, Gangopadhyay J, Yamazaki T, Winkelbauer-Hurt ME, Yin S, Eliasse Y, Adams E, Shaw CE, Reed R (2015) U1 snRNP is mislocalized in ALS patient fibroblasts bearing NLS mutations in FUS and is required for motor neuron outgrowth in zebrafish. *Nucleic Acids Res* 43: 3208–3218
- Zhang Z, Lotti F, Dittmar K, Younis I, Wan L, Kasim M, Dreyfuss G (2008) SMN deficiency causes tissue-specific perturbations in the repertoire of snRNAs and widespread defects in splicing. *Cell* 133: 585–600
- Zhou H, Mangelsdorf M, Liu J, Zhu L, Wu JY (2014) RNA-binding proteins in neurological diseases. *Sci China Life Sci* 57: 432–444
- Zhou Y, Liu S, Liu G, Ozturk A, Hicks GG (2013) ALS-associated FUS mutations result in compromised FUS alternative splicing and autoregulation. *PLoS Genet* 9: e1003895
- Zhou Z, Licklider LJ, Gygi SP, Reed R (2002) Comprehensive proteomic analysis of the human spliceosome. *Nature* 419: 182–185
- Zinszner H, Sok J, Immanuel D, Yin Y, Ron D (1997) TLS (FUS) binds RNA in vivo and engages in nucleo-cytoplasmic shuttling. *J Cell Sci* 110: 1741–1750